Proc. NIPR Symp. Antarct. Meteorites, 1, 65–101, 1988

QINGZHEN AND YAMATO-691: A TENTATIVE ALPHABET FOR THE EH CHONDRITES

A. EL GORESY[1], Hideo YABUKI[2], K. EHLERS[1], D. WOOLUM[3] and E. PERNICKA[1]

[1]*Max-Planck-Institut für Kernphysik, Postfach 103980, 6900 Heidelberg, F.R.G.*
[2]*The Institute of Physical and Chemical Research, Wako 351-01*
[3]*California State University, Fullerton, California 92634, U.S.A.*

Abstract: Petrological investigations of unequilibrated EH chondrites revealed the presence of three subgroups. They are identified based on the presence of different concentrations of MnS in niningerite. These differences were produced by partitioning of Mn between niningerite and enstatite as a result of different f_{S_2} and f_{O_2} during their formation. In order of increasing MnS-contents and hence increasing f_{S_2} and decreasing f_{O_2} these groups are: (A) Yamato (Y)-691 and Abee, (B) Indarch, and (C) Yamato-74370, South Oman, Qingzhen, Kota Kota, Kaidun III, and St. Marks. In the third subgroup the meteorites follow an equilibration and evolution sequence; Y-74370 the most primitive and St. Marks the most equilibrated. Y-691 is the most primitive in its subgroup. Differences in the chemical compositions of minerals in Y-691 and Qingzhen reveal a dichotomy in the compositions of niningerite, djerfisherite, kamacite, and perryite. Niningerites in Y-691 contain the least MnS (3.6–6.7 mole%) and counterparts in Qingzhen the most (12–14 mole%). K/Na ratios in djerfisherite are lower in Qingzhen than in Y-691. The Si concentration in kamacite in Qingzhen is higher than in Y-691. Ni in perryite in Qingzhen is higher than in Y-691.

Na and K are highly fractionated between two sulfide lithologies. Na resides mainly in chondrules in caswellsilverite, in a Cl-bearing glass in the chondrules, and in Cr-rich sulfides in the matrix. In contrast, K is confined to djerfisherite, which occurs only in sulfide-rich objects in the matrix, and is highly depleted in chondrules. Two new layer structure minerals were discovered in Y-691: (a) Na-Cu-Cr-sulfide with the general formula (NaCu) CrS_2, and (b) a Na-Cu-Zn-Cr-sulfide.

An evolution scheme was constructed for the EH chondrites in the solar nebula and in their parent bodies. Niningerite and oldhamite condensed first and probably acted as nucleation sites for condensing sulfides, metals and silicates. Both minerals are abundant in chondrules, indicating that chondrule formation preceded all other sulfide- and metal-rich objects. For the first time, planetary metamorphic events were recognized. The Qingzhen Reaction, a breakdown of djerfisherite to troilite, covellite, idaite, bornite, and other unidentified phases, was discovered in Qingzhen and Y-691. Thermal episodes took place in the parent bodies at 1.4 Ba (Qingzhen), and 800 Ma (Y-691). Reverse zoning in niningerite indicates that Fe diffused from troilite to niningerite during the thermal event. In Y-691 sphalerite also formed during the metamorphic episode due to mobilization of Zn (and other volatiles). EH chondrites condensed in a chemically inhomogeneous region of the solar nebula where considerable variations in sulfur and oxygen fugacities existed.

1. Introduction

The enstatite chondrites are the most reduced group among chondritic meteorites. Elements which are typically lithophile in carbonaceous and ordinary chondrites display either siderophile or chalcophile behavior in enstatite chondrites. For example, most of the Ca is present as oldhamite (CaS) and a considerable amount of Mg is incorporated either in niningerite ((Mg Fe Mn)S) or in ferroan alabandite ((Mn Fe Mg)S), in EH and EL chondrites, respectively. Iron-nickel contains appreciable amounts of alloyed Si and the Si-rich phase perryite $((Ni\ Fe)_5\ (Si\ P)_2)$. This unusual behavior of typically lithophile elements is considered a result of very low f_{O_2}, which must have prevailed during the formation of these meteorites in the solar nebula (LARIMER and BARTHOLOMAY, 1979) and during their further evolution in their parent bodies (EL GORESY, 1985; EL GORESY *et al.*, 1986).

Based on differences in Fe/Si *versus* Mg/Si ratios, SEARS *et al.* (1982) recognized two groups in the enstatite chondrite clan: (a) EH (high iron), and (b) EL (low iron). Differences in the abundances in the siderophile and chalcophile elements between EH and EL chondrites were also reported by SEARS *et al.* (1982) and confirmed by KALLEMEYN and WASSON (1986). Both reports agree that these differences cannot have resulted from metamorphic processes. Hence, it is quite certain that the EL chondrites were not generated by metamorphism of EHs.

The unequilibrated members of the EH chondrites are enigmatic and the least understood among the enstatite chondrite clan. KALLEMEYN and WASSON (1986) indicate that there are no differences in the abundances of many siderophile elements between EH3, and EH4, 5 chondrites. Apart from the differences in elemental abundances of siderophiles and chalcophiles (WEAKS and SEARS, 1985; KALLEMEYN and WASSON, 1986) the majority of the EH chondrites, specifically the unequilibrated members, display a remarkable fractionation of Na and K between two different sulfide lithologies (EL GORESY *et al.*, 1983, 1986). Potassium is incorporated in djerfisherite, $(K_3Cu(Fe\ Ni)_{12}\ (S\ Cl)_{14})$ while sodium is associated with Cr in several sulfide phases including caswell-silverite, daubreelite, and at least two new Na-Cu-Cr- and Na-Cu-Zn-Cr-sulfides (EL GORESY *et al.*, 1983, 1986). Na is also present in Cl-rich silicate glass in chondrules. In contrast, in all EL members and a few of the EH group Na and K display lithophile behavior.

Qingzhen and Y-691 are considered to be the least equilibrated among the EH group (OKADA *et al.*, 1975; EL GORESY *et al.*, 1983, 1986; RAMBALDI *et al.*, 1983). Both meteorites were classified as EH3 due to the broad ferrosilite range in their enstatites and due to the presence of glass in their chondrules. Qingzhen and Y-691 also show low ^{40}Ar-^{39}Ar ages: Qingzhen 2.88 Ba, Y-691 800 Ma (MÜLLER and JESSBERGER, 1985; HONDA *et al.*, 1983). These low ages must have resulted from post accretionary events. Another related problem is a meaningful interpretation of the relative abundance patterns of chalcophile elements among the EH chondrites in relation to their petrographic characteristics. A major uncertainty is caused by the effects of terrestrial weathering. Oldhamite is quite sensitive to weathering and reacts readily with water. Leaching of this mineral will severely affect the Ca and REE abundances in the meteorites. It has been also postulated that djerfisherite and caswellsilverite are easily leached

(GROSSMAN *et al.*, 1985). KALLEMEYN and WASSON (1986) also believe that low abundances of Cr, Mn, Na, K, and Zn may have resulted from weathering. Admittedly, there are some expected changes in elemental abundances due to terrestrial weathering. However, there is disagreement between conclusions drawn from chemical investigations and petrographic evidence. It should be remembered that different sulfides respond differently to causes of weathering. Resistance to weathering depends mainly on crystal structures rather than on the solubilities of elements.

In this paper we will present results of petrographic investigations of Qingzhen and Y-691. We will classify the various types of clasts and fragments, and document characteristics of their mineral assemblages. We will also compare the assemblages and trends in mineral compositions with those of other members of the EH group. To identify the metamorphic episodes experienced by the meteorites the chalcophile behavior of Na and K will be discussed with special attention given to mineral assemblages containing djerfisherite and caswellsilverite. In this context we consider the origin of (OH)- and (H_2O)-bearing minerals to be unresolved so far. The interpretations given by some scholars supporting a terrestrial origin are based solely on observations in *enstatite achondrites*. In addition, there is no *a priori* evidence for exclusively terrestrial weathering processes. Another important quest is the genetic relationship between the various members of the EH group if the petrological and chemical data are capable of resolving differences, similarities, and possible evolution trends.

2. Analytical Procedure

Petrographic investigations were performed both using transmitted and reflected light. A detailed SEM survey of the sections was conducted to delineate the complex textural characteristics of the different clasts and fragments. SEM investigations were carried out with a Cambridge 180S scanning electron microscope with a Si(Li) detector (143eV resolution) and a Tracor Northern 5500 system. Quantitative analyses of the mineral phases were performed with an automated, computer controlled, SEMQ electron microprobe with wavelength dispersive spectrometers. The analyses were corrected for background, beamdrift, and matrix effects using the procedures of BENCE and ALBEE (1968), and ALBEE and RAY (1970) for silicates, and conventional ZAF corrections for metals, sulfides, and phosphides. A special analytical procedure and a peak deconvolution program was applied to correct for X-ray overlaps of K_β on the K_α lines of the successive elements of higher atomic number (*e.g.* Ti-V, Cr-Mn, Mn-Fe, Fe-Co, Co-Ni, Ni-Cu, Cu-Zn, K-Ca). Pure synthetic Na-free daubreelite was used as an internal standard to monitor low Na concentrations in meteoritic daubreelite and other Cr-rich sulfides.

3. Major and Trace Element Chemistry

Major and trace element chemical compositions were determined for Qingzhen only, because a sample of Y-691 was not available for chemical investigations. Chemical data on Y-691 were recently reported by KALLEMEYN and WASSON (1986). The chemical composition of Qingzhen was determined by XRF and NAA on separate aliquots of

Table 1. XRF analysis of the non-magnetic fraction in Qingzhen.

	Weight percent
SiO_2	40.75
Al_2O_3	1.39
CaO	1.28
MgO	22.9
FeO	19.5≙15.2 Fe

Table 2. NAA results of magnetic and non-magnetic fractions in Qingzhen.

Element	Magnetic	Non-magnetic
Fe	69.8%	15.1%
Ni	4.38%	1.03%
Co	0.241%	0.0228%
Na	0.281%	0.676%
K	—	741 ppm
Sc	2.44 ppm	8.48 ppm
Mn	—	0.222%
Zn	—	231 ppm
Se	—	32 ppm
Ir	1.87 ppm	0.24 ppm
Au	1.10 ppm	0.10 ppm

Table 3. Bulk composition of Qingzhen calculated from element concentrations in the magnetic and non-magnetic fractions.

Measured		Calculated	
SiO_2	32.5%	FeS	15%
Al_2O_3	1.11%	Fe_{met}	23.5%
CaO	1.02%		
MgO	18.2%		
Fe_{tot}	32.6%		
Ni	2.1%		
Co	0.093%		
Na_2O	0.74%		
K_2O	0.071%		
Cr_2O_3	0.43%		
MnO	0.23%		
Sc	6.55 ppm		
Se	25.9 ppm		
Zn	184 ppm		
Ir	0.76 ppm		
Au	0.42 ppm		
Fe/Si=1.08	atom. ratios		
Mg/Si=0.83			

the meteorite. 2.777 g of Qingzhen were crushed and separated into two parts by a hand magnet: (1) a non-magnetic fraction, consisting mainly of silicates and sulfides (mainly troilite) weighed 1.888 g, and (2) a magnetic fraction consisting of metals, sulfides, and minor silicates, weighed 0.889 g. The non-magnetic fraction was ground to a grain size of <50 microns. 400 mg of this powder were prepared for XRF analysis by fusion in $Li_2B_4O_7$ according to the procedure described by NORRISH and HUTTON (1968). Another aliquot of 76 mg of the non-magnetic fraction was irradiated with thermal neutrons to determine Na, K, Sc, Mn, Fe, Co, Ni, Zn, Se, Ir, and Au. The results are given in Tables 1 and 2. Note the excellent agreement between XRF and NAA results for Fe. The major element composition is shown in Table 3. The Fe/Si and Mg/Si ratios places Qingzhen clearly in the EH group. Qingzhen has the highest measured Fe/Si ratio among EH chondrites. The major chemical composition determined by us for Qingzhen compares very well with the recent data of KALLEMEYN and WASSON (except for Fe). We obtain an Fe content of 32.6% compared to 29.9% by KALLEMEYN and WASSON (1986).

4. Petrography

Qingzhen and Y-691 share many petrographic characteristics with other members of the EH group *e.g.* Y-74370, ALHA77294, Kota Kota, Kaidun III, Indarch, and St. Marks. Textural relationships in Indarch and St. Marks are similar but slightly different from those of Qingzhen and Y-691. The mode of occurrence of metals and sulfides in the EH group is of special interest. Metals (kamacite and perryite), sulfides (troilite, daubreelite, djerfisherite, oldhamite, niningerite,...etc.), and schreibersite occur usually in multiphase and complex rounded objects, clasts, and fragments (Fig. 1). These minerals, specifically the metals, are present also in the interstices of silicate

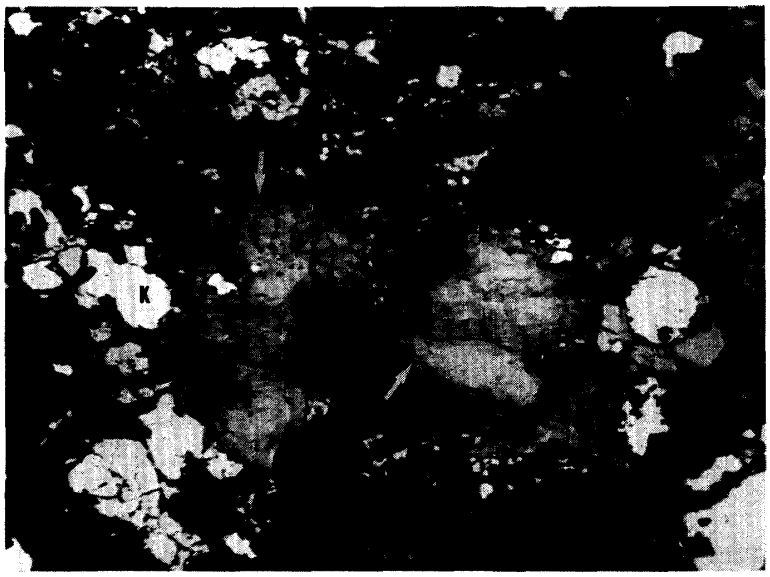

Fig. 1. A low magnification photograph in reflected light of Qingzhen. The figure displays metal (K) and Na-Cr-sulfide clasts (arrows). Length of photograph 1.5 mm.

minerals in the matrix. The abundance of fragments and clasts in the unequilibrated members like Qingzhen, Y-691, and Y-74370 are, however, much higher than in St. Marks and Indarch (EH4). There is also a gradual change in the mode of intergrowth of graphite and kamacite from EH3 (*e.g.* Y-691) to EH4 members like Indarch, Kaidun III, and St. Marks. Two distinct types of intergrowths are encountered. Their relative abundances changes from EH3 (Qingzhen, Y-691) to EH4 (Kaidun III, St. Marks, and Indarch). These two types are: (a) Graphite spherules which grade to cliftonite type texture, and (b) graphite lamellae of variable sizes preferentially oriented along the octahedral planes of kamacite. The first type is dominant in the EH3 and the second type in the EH4, specifically in Kaidun III and St. Marks. The occurrence of graphite lamellae in kamacite along with perryite in St. Marks was observed by RAMDOHR (1973). The perryite-kamacite intergrowths are also quite complex with various textures in the same meteorite.

Table 4. Mineral assemblages and clast types in Qingzhen and Y-691.

Clast type	Mineral assemblage	Qingzhen	Y-691	Remarks
1. Oldhamite-niningerite clasts	CaS, niningerite, Fes; less abundant: djerfisherite, $NaCrS_2$, secondary FeS	+	+	Breakdown textures of djerfisherite are quite advanced.
2. Troilite-daubreelite clasts	FeS, daubreelite, hydrated NaCr sulfides	++	+	Hydrated NaCr sulfides are intimately intergrown with daubreelite (Qingzhen).
3. Multiphase metal sulfide spherules	Niningerite, CaS, kamacite, perryite daubreelite, $(FeNi)_3P$, djerfisherite, hydrated NaCr sulfides, graphite	+	+	CaS and niningerite occupy usually the cores of the spherules.
4. NaCr sulfide clasts	Hydrated NaCr sulfides daubreelite, smythite, greigite	+	−	Hydrated NaCr sulfides are oriented along (111) and (0001) of daubreelite. Daubreelite also oriented with its (111) along the basal plane of the hydrated sulfides.
5. Metal graphite clasts	a. kamacite, perryite, graphite, spherules	+	+	Graphite spherules are presumably breakdown product of cohenite.
	b. kamacite, perryite, graphite lamellae, FeS	+	+	Graphite lamellae in kamacite formed by exsolution of graphite from γFe or kamacite.
6. Djerfisherite veins	Djerfisherite, secondary FeS	+	−	Incipient breakdown of djerfisherite.
7. Kamacite, djerifisherite clasts	Kamacite, perryite, djerfisherite, secondary ZnS	−	+	Advanced breakdwon of djerfisherite. ZnS displays the same frothy texture like secondary FeS.
8. Na-Cu-Zn sulfide-rich clasts	New (NaCu) CrS_2, new (NaCuZn) CrS_2, FeS, perryite, kamacite, $(FeNi)_3P$	−	+	(NaCuZn) CrS_2 envelopes (NaCu)CrS_2 along grain boundaries and cracks.
9. Sphalerite-troilite clasts	Primary ZnS, niningerite, FeS, kamacite, perryite, $(FeNi)_3P$	+	+	Fine-grained ZnS intergrown with troilite and schreibersite (Qingzhen). Coarse-grained ZnS with troilite and niningerite (Y-691).
10. Low temperature sulfide patches	Greigite, smythite	+	+	Both minerals occur in convoluting veins.

In this report we will argue that the two graphite intergrowth textures were produced by different mechanisms at different temperatures. The textures produced are evidently a function of the Ni and C contents of the Fe Ni alloys and are presumably linked to the formation of perryite. All these features, along with the mineral compositions of each meteorite, should help to set a tentative evolution scheme for the EH group.

A distinct distribution pattern for metals and sulfides between chondrules, clasts, fragments, and matrices was observed. The total amount of metals and sulfides in chondrules is markedly lower than in the matrices and clasts. In chondrules niningerite is the most abundant sulfide. It occurs usually with oldhamite and minor troilite. In Qingzhen, caswellsilverite seems to be relatively enriched in chondrules compared to its abundance in the matrix. In contrast, djerfisherite is restricted to the matrix and metal-sulfide clasts and was never observed in chondrules. This mode of occurrence offers a straightforward explanation for the depletion of K in chondrules. Consequently, this depletion is a primordial feature and did not result from terrestrial weathering as has been postulated by GROSSMAN *et al.* (1985). The silicate glass in the chondrules is also depleted in K. The Na/K ratios in the glass in the chondrules ranges between 60 and 300 (see also pages 81 and 95) thus supporting a primordial K depletion in the chondrules. In many EH4s djerfisherite is very rare (St. Marks and Kaidun III) and in Indarch it appears to be absent.

Metals and most of the sulfides are associated in multiphase clasts or spherules. Each type of object contains a specific assemblage (Table 4). Some of these assemblages presumably store records of early nebular processes. For example, niningerite-oldhamite clasts may represent the refractory portion of nebular condensates similar to CAIs in C2 and CV3 chondrites. The textural characteristics of the various metal- and sulfide-rich objects in Qingzhen and Y-691 may reflect different sequences of events during the evolution of the meteorites in the solar nebula and in their parent bodies.

5. Textural Characteristics of Qingzhen and Yamato-691

The distribution of the various sulfides and metal alloys among the different clast types follows a distinct pattern. This is well reflected in the complex assemblages briefly presented in Table 4. Likewise, the textural relations of the individual clasts and fragment types are distinct and hence indicate specific genetic processes. The sequence of the clast types depicted in Table 4 does not reflect the relative abundance of these objects in the two meteorites. This sequence rather reflects the genetic importance of an assemblage type, as interpreted from the petrographic evidence. The number of constituents in a clast type is not always identical in the two meteorites. Similarities and differences will be treated in detail in the following section.

5.1. Clasts and fragments

5.1.1. Oldhamite-niningerite clasts

They consist usually of large idiomorphic to rounded grains of niningerite with smaller and less abundant crystals of oldhamite (Fig. 2). This association gains genetic importance in view of the thermodynamic calculations by LATTIMER *et al.* (1978) and

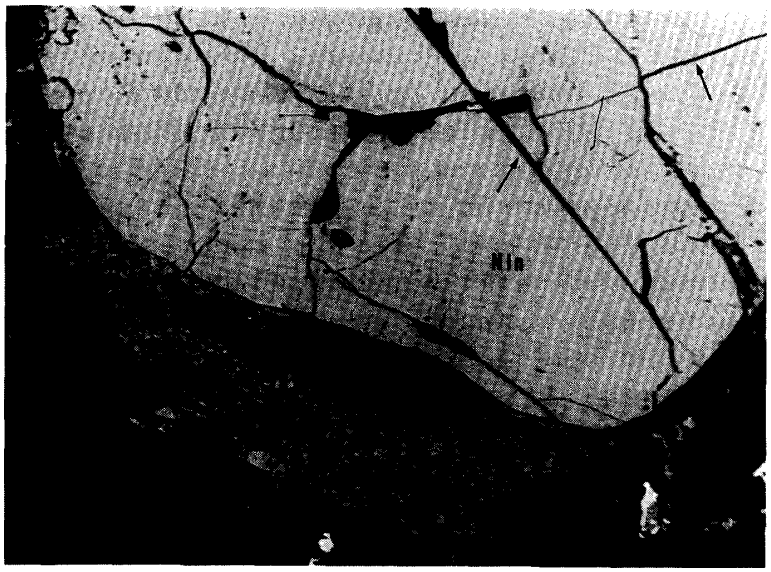

Fig. 2. A detail of a niningerite-oldhamite clast from Qingzhen. Rounded grain of niningerite (Nin) with well developed cleavage along (111) directions (arrows). The grain is covered with a djerfisherite grain (Djr) with advanced Qingzhen Reaction. Length of photograph 300 microns.

LARIMER and BARTHOLOMAY (1979) which indicate that CaS and MgS were among the earliest condensates from a solar gas with high C/O ratio (>1.5). The assemblage also gains importance in view of its temporal and spatial evolution in the solar nebula based on the following textural evidence: (a) In chondrules, clasts, and matrices of both meteorites oldhamite and niningerite are often intergrown together (Table 4). (b) Both minerals contain numerous inclusions of schreibersite spherules, thus suggesting simultaneous formation around these spherules. In Qingzhen caswellsilverite also contains the same type of spherules when associated with niningerite and oldhamite (Fig. 3). (c) Schreibersite spherules are also encountered in coexisting niningerite and oldhamite present in other metal-sulfide clasts, *e.g.* in multiphase metal-sulfide spherules. This feature suggests a common source for the oldhamite-niningerite pair or a common formation mechanism for the pair in all clast types in which they show this texture.

5.1.2. Troilite-daubreelite clasts

This clast type consists of major troilite with daubreelite and occasionally hydrated Na-Cr sulfides. The amount of daubreelite varies widely from few thin lamellae to coarse tabular masses which may reach 40% of the clasts by volume. The hydrated Na-Cr sulfides are usually confined to the daubreelite lamellae and are crystallographically oriented with their basal plane along the octahedral planes of daubreelite (Fig. 4). The genetic importance of this assemblage is indicated by: (a) A Na/Cr geochemical coherency in daubreelite and the hydrated Na-Cr sulfides, (see section on mineral chemistry) and (b) formation of the troilite-daubreelite pair as a result of the invariant reaction

$$2FeS + 2CrS \rightleftharpoons FeCr_2S_4 + \alpha Fe$$

(EL GORESY and KULLERUD, 1969). Caswellsilverite was not encountered in this clast type.

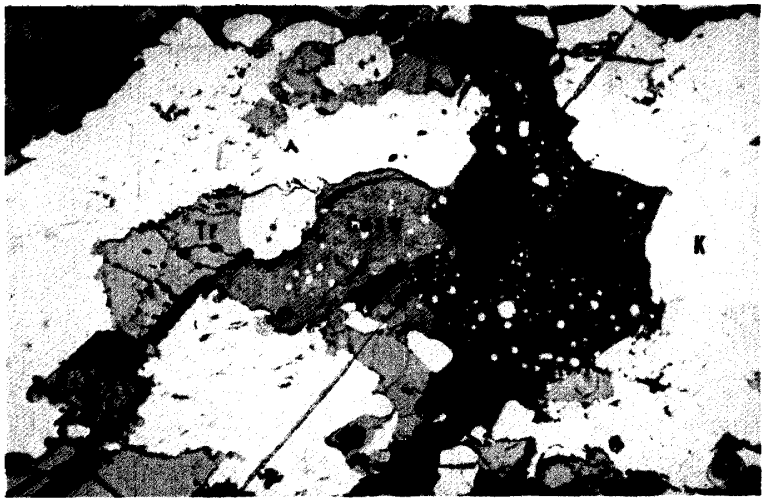

Fig. 3. Niningerite (Nin), oldhamite (Old), and caswellsilverite (green Casw) with schreibersite spherules (arrow). The assemblage is enclosed in metal (K) and troilite (Tr) in a chondrule in Qingzhen. Length of photograph 200 microns.

Fig. 4. Daubreelite (D) lamellae in troilite (Tr) from Qingzhen. Mineral A (arrows) occurs in daubreelite oriented parallel to (111) directions. Length of photograph 200 microns.

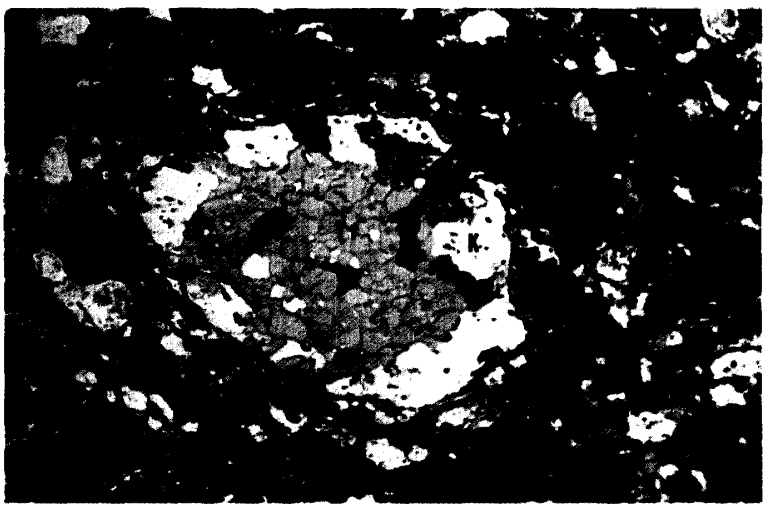

Fig. 5. A color photograph of a complex sulfide-metal spherule from Qingzhen. Oldhamite and niningerite (gray) occupy the core. Troilite (Tr) displays triple junctions. Djerfisherite (Djr) and metal (K) occur at the outer margins. Length of photograph 700 microns.

5.1.3. Multiphase metal-sulfide spherules

This type is one of the most abundant in all unequilibrated EH chondrites. The highest abundance was encountered in Qingzhen, Y-691, Y-74370, and Kota Kota. Its abundance decreases in the EH4s Kaidun III, Indarch, and St. Marks. Textural relationships are complex (Fig. 5). Minerals present include niningerite, oldhamite, troilite, schreibersite, kamacite, perryite, djerfisherite, hydrated Na-Cr sulfides, graphite spherules, . . . etc. Niningerite and oldhamite occupy the cores of the spherules whereas kamacite and djerfisherite usually reside in the outer portions (Fig. 5). This suggests that both niningerite and oldhamite may have acted as nucleation sites for accretion of other sulfide and metal constituents in the solar nebula. Troilite is the most abundant mineral and usually displays a polycrystalline texture with 120° triple junctions. In Qingzhen perryite occurs as a thin veneer between troilite and kamacite. Niningerite and oldhamite contain numerous inclusions of schreibersite spherules.

5.1.4. Hydrated Na-Cr sulfide clasts

The minerals encountered are two hydrated Na-Cr sulfides, daubreelite, and minor troilite. The clasts usually display ragged edges suggesting that they are fragments broken from larger Cr-sulfide-rich objects. The two Na-Cr sulfides have reflectivities and reflection colors which are distinctly different from those of caswellsilverite.

The first is a bright gray phase (herein designated phase A) with a reflectivity slightly lower than that of daubreelite, and the second is a dark gray component with low reflectivity (designated phase B). Both phases are intimately intergrown with each other and with daubreelite (Fig. 6). They usually occur as thin lamellae alternately intergrown with each other (Fig. 6). In some cases phase A forms coherent patchy areas with well developed twin lamellae (Fig. 7). Daubreelite is also present as fine lamellae alternately intergrown with A and B (Fig. 7). Both A and B are highly anisotropic suggesting that both are layer-structure minerals. In some cases closely spaced twin lamellae are present thus strongly suggesting formation during preterrestrial shock events. This is also supported by the presence of undulose extinction and shock twin lamellae in the coexisting troilite.

5.1.5. Metal-graphite clasts

This type consists of major kamacite with minor amounts of graphite, perryite, troilite, and schreibersite. We identified two distinct subtypes depending on the kamacite-graphite intergrowth textures: (a) Metal clasts with graphite spherulites with radially oriented graphite flakes. Usually the radial texture is poorly developed perhaps because the graphite is either fine-grained or amorphous. Spherulitic graphite is abundant in Qingzhen, Y-691, and Y-74370. It is rare in Indarch, St. Marks, and Kaidun III. (b) Metal clasts with well oriented graphite lamellae The graphite lamellae are oriented along (111) directions of kamacite (Fig. 8). The amount of graphite may reach as much as 30% by volume of the kamacite-graphite intergrowth (Fig. 8). Idiomorphic enstatite crystals occasionally intersect the graphite lamellae, thus suggesting that the enstatite preceded the intergrowth. This type is abundant in the EH4s specifically in St. Marks and Kaidun III and is very rare in all EH3s. Small patches of perryite were also found as inclusions in kamacite usually caught between two successive graphite lamellae. In both Qingzhen and Y-691 perryite is confined to either the kamacite-troilite interface (Qingzhen), or kamacite alone (Y-691). In the latter perryite occurs as small grains

Fig. 6. An intimate intergrowth of daubreelite lamellae (D), mineral A (A) and mineral B (B) in Qingzhen. Length of photograph 100 microns.

Fig. 7. An intimate intergrowth of daubreelite (D), mineral A (A), and mineral B (B) in Qingzhen. Both A and B display shock-induced twin lamellae. Daubreelite lamellae are highly folded.

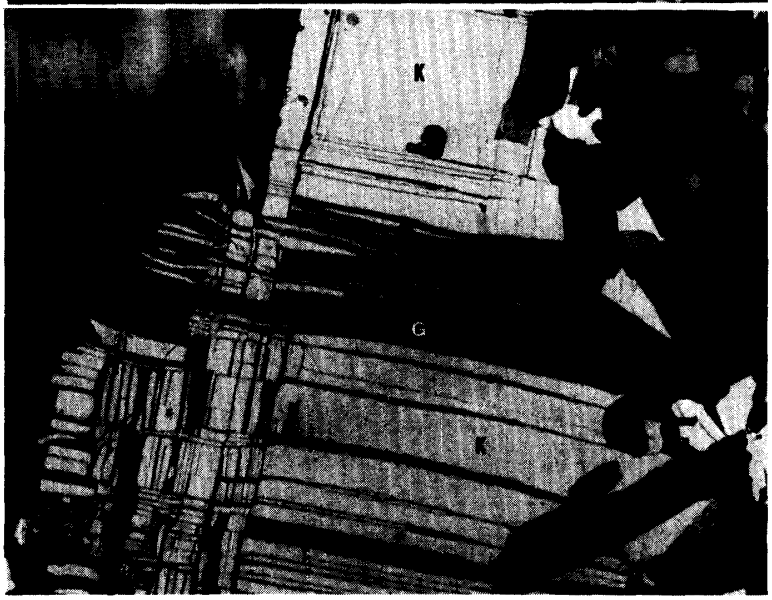

Fig. 8. Well oriented graphite lamellae (G) in kamacite (K) in St. Marks meteorite. Graphite also contains fine kamacite lamellae.

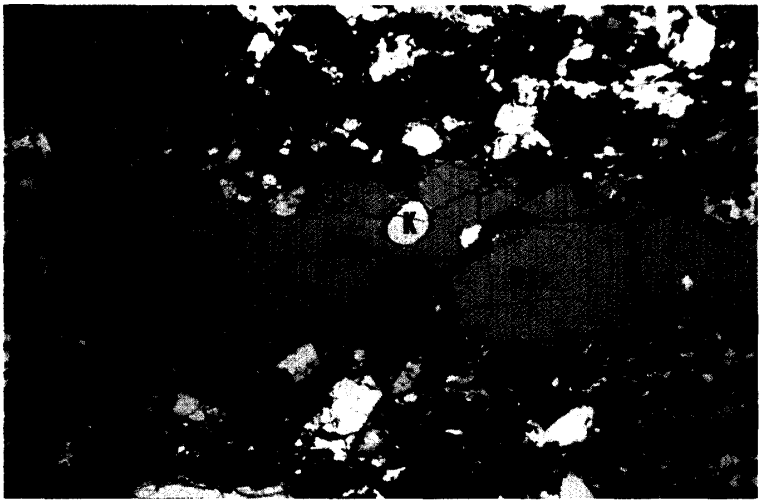

Fig. 9. A large djerfisherite grain (Djr) in Qingzhen. The grain shows incipient Qingzhen Reaction (arrows) and an inclusion of kamacite (K). Length of photograph 1.5 mm.

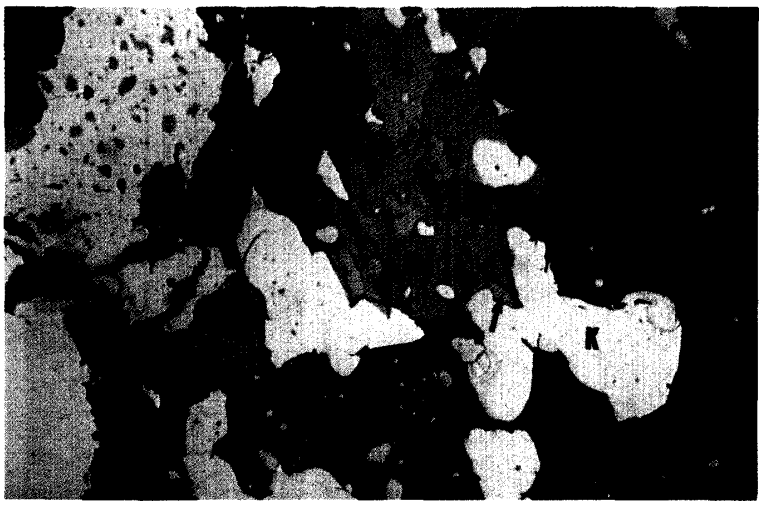

Fig. 10. A color photograph of a complex intergrowth involving Na-Cu-Cr-sulfides in Y-691. New Na-Cu-Cr-sulfide (Cu) with lamellae of Na-Cu-Zn-Cr-sulfide (gray), and a small grain of caswellsilverite (arrow). The assemblage is accompanied by daubreelite, kamacite (K), troilite (Tr), and niningerite (Nin). Length of photograph 200 microns.

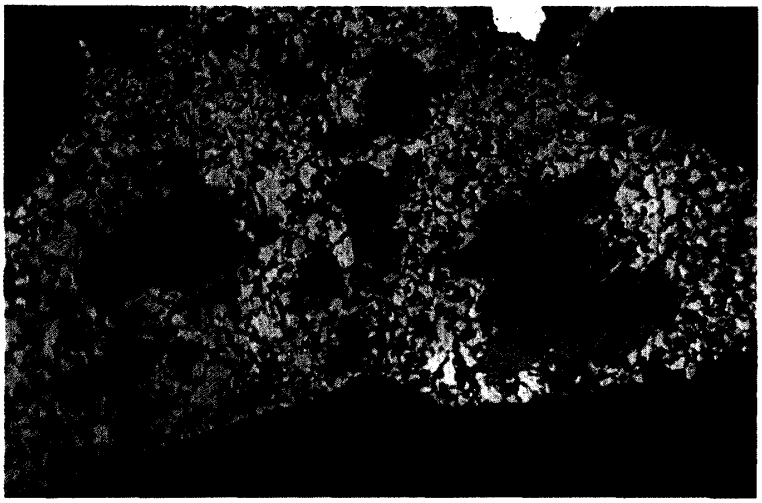

Fig. 13. A color photograph of a highly advanced Qingzhen Reaction in Qingzhen. Djerfisherite (Djr) is surrounded by fine-grained secondary troilite (Tr). The djerfisherite is leaning on a niningerite grain (Nin). Length of photograph 200 microns.

overgrown on kamacite. In many cases perryite was encountered, however, as exsolution lamellae oriented in kamacite along three crystallographic directions. Evidently the graphite lamellae preceded the perryite formation.

5.1.6. Djerfisherite veins and fragments

One of the most striking features of EH3s is that djerfisherite is confined to clasts, fragments, spherules, and veins in the matrices and was never encountered in chondrules. In Qingzhen djerfisherite is mainly present in large millimeter-sized fragments or veins in the fine-grained matrix (Fig. 9). The veins and fragments either consist entirely of djerfisherite or contain subordinate amounts of rounded blebs of kamacite (Fig. 9). Large specks of djerfisherite are also found together with oldhamite-niningerite clasts in Qingzhen. Large millimeter-sized masses of djerfisherite occur as well in Y-691 but are much less abundant than in Qingzhen. Djerfisherite in Qingzhen and Y-691 displays a breakdown texture described by EL GORESY as the "*QINGZHEN REACTION*". These breakdown textures will be described in a separate section of this report.

5.1.7. Kamacite-djerfisherite clasts

This fragment type is quite abundant in Y-691 and was not found in Qingzhen. Kamacite is usually the major phase accompanied by djerfisherite relicts of the Qingzhen reaction, primary troilite, and secondary porous troilite formed by the Qingzhen reaction. Minor phases include perryite and spherulitic graphite. Small inclusions of porous sphalerite, presumably formed by the Qingzhen reaction are also present as inclusions in porous troilite.

5.1.8. Na-Cu-Cr-Zn rich multisulfide clasts

The textural relations of this type are quite complex, and have been encountered only in Y-691. The mineral assemblage includes niningerite, oldhamite, kamacite, perryite, troilite, schreibersite, caswellsilverite, and at least two new layer structure minerals chemically related to caswellsilverite. An overall view of such a clast is shown in Fig. 10. The major layer structure mineral is a brownish strongly pleochroic Na-Cr-Cu-sulfide (Fig. 10). It usually coexists with minor caswellsilverite (Fig. 10) and a gray strongly pleochroic mineral with optical properties similar to phase B found in Qingzhen. The gray mineral in Y-691 is, however, chemically distinct from phase B. It is a Na-Cu-Zn-Cr-sulfide (see Section 6 on mineral chemistry). High magnification BSE imaging with the SEM indicates that this mineral occurs as thin veneers in cracks, around the Na-Cr-Cu-sulfide or as reaction rims around it (Fig. 11). This suggests that the mineral was formed in a late event as a result of Zn mobilization and precipitation around the Na-Cu-Cr-sulfide.

5.1.9. Sphalerite-troilite fragments and clasts

In general this type resembles the previous one. It is, however, distinguished by the presence of major sphalerite. As in the other clast types, troilite is always polycrystalline with triple junctions. Sphalerite is present as large ($>$120 microns) grains intimately intergrown with troilite and kamacite. Both new minerals encountered in the previous type were also observed in this clast type.

5.1.10. Low temperature sulfide patches

This type was found in both Qingzhen and Y-691. It is characterized by the presence of highly convoluted fine-grained stringers of troilite-like sulfide phases (Fig. 12).

Most of the sulfides are optically isotropic and the chemical analyses revealed compositions suggestive of greigite and/or smythite. The presence of this assemblage is intriguing in view of the low temperature upper stability limits of these minerals ($<75°C$) (KISSIN, 1974).

5.2. The Qingzhen Reaction

This breakdown was discovered by EL GORESY *et al.* (1983) in the Qingzhen meteorite. Djerfisherite grains, specifically those in large clasts and veins, were found to display mottled troilite at their rims (Fig. 9). The amount of this troilite varies considerably from grain to grain. Gradations between incipient reaction and advanced decomposition occur in the same sample (Figs. 9 and 13). In the latter cases, djerfisherite is encountered as islands or relicts enclosed in the mottled troilite (Fig. 13). The breakdown products include troilite, an unknown K-bearing mineral, and other

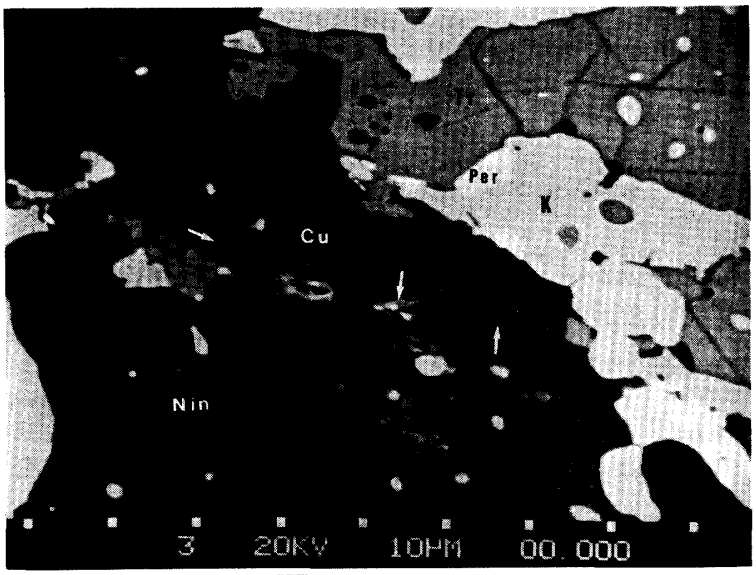

Fig. 11. SEM photograph of new Na-Cu-Cr-sulfide (Cu) from Y-691. The new Na-Cu-Cr-sulfide is surrounded by thin rims of Na-Cu-Zn-Cr-sulfide (arrows). The assemblage is accompanied by niningerite (Nin), troilite (Tr), kamacite (K), and perryite (Per).

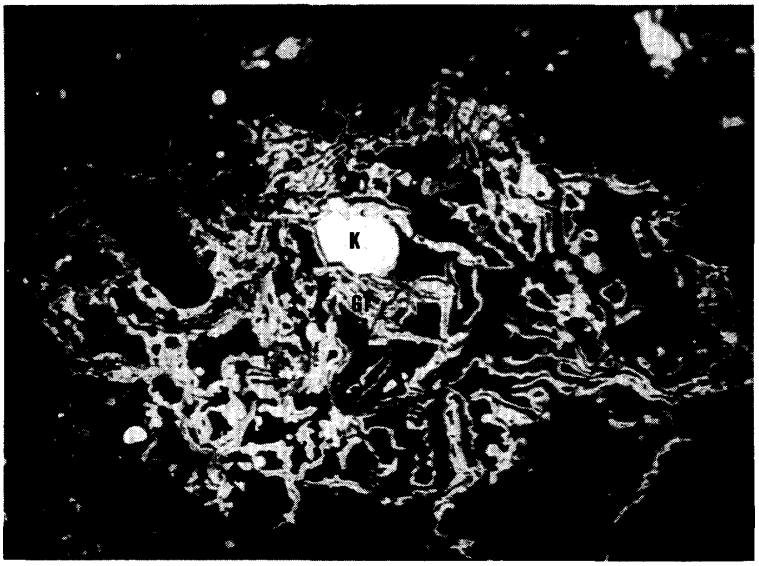

Fig. 12. Highly convoluted veins of greigite and/or smythite (Gr) in Qingzhen. Length of photograph 50 microns.

unidentified phases. It was impossible to identify the breakdown products due to their extremely fine-grained nature. In Y-691 the reaction is much more pervasive (Fig. 14). In contrast to Qingzhen, the secondary troilite in Y-691 is coarse-grained (Fig. 14). Djerfisherite is usually present as bizarre-shaped patches in highly porous secondary troilite (Fig. 15). Large djerfisherite grains still maintain large intact areas in their cores. They are, however penetrated by veins of secondary troilite. Detailed studies with a SEM showed the frothy nature of the porous troilite thus indicating that volatile species were involved in the breakdown reaction (Fig. 15). In some cases a fine intergrowth of idaite, bornite, and individual covellite were found in the porous troilite (Figs. 16 and 17). Figures 16 and 17 display clearly the typical basal cleavage of the idaite crystals. These Cu-bearing sulfides were formed by the Qingzhen reaction upon release of Cu from the decomposed djerfisherite. Sphalerite was also encountered as an accessory phase in the secondary troilite. This is quite surprising because djerfisherite does

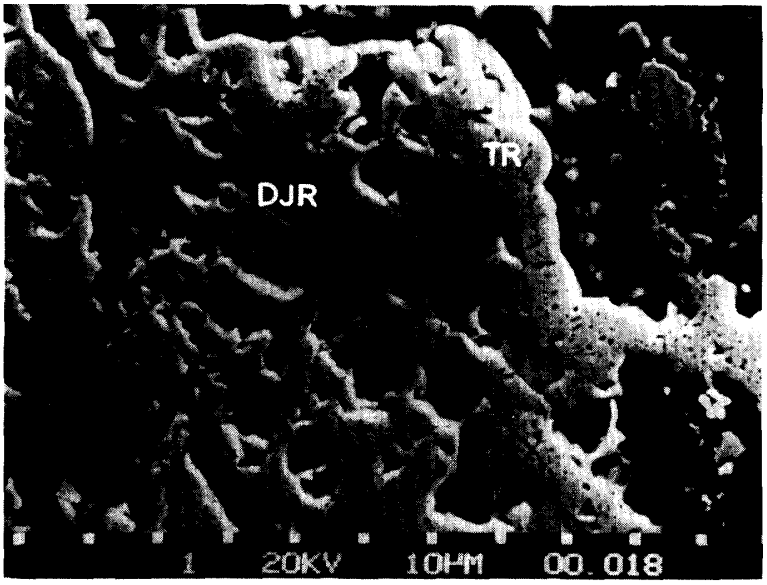

Fig. 14. A SEM photograph of advanced djerfisherite breakdown in Y-691. Djerfisherite relicts (Djr) are surrounded by frothy secondary troilite.

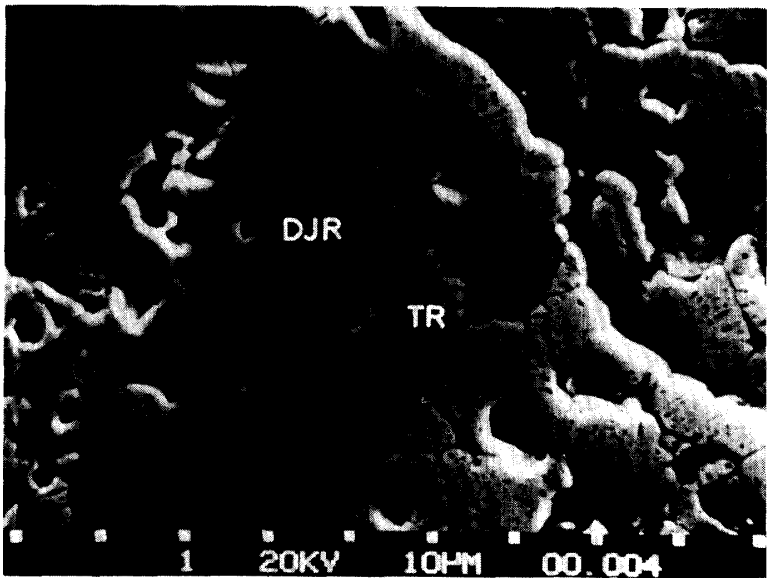

Fig. 15. A SEM detail of the Qingzhen Reaction products in Y-691. Secondary troilite (Tr) displays the spongy texture due to the presence of gas bubbles (black rounded holes).

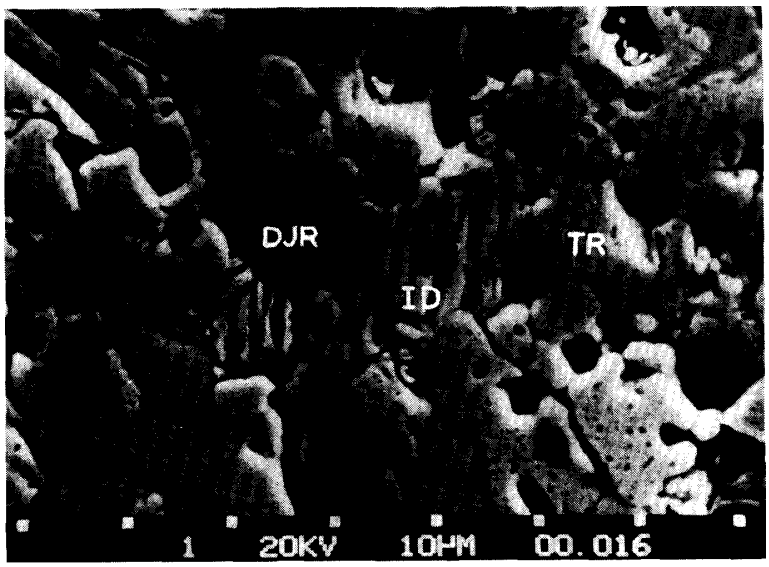

Fig. 16. A pervasive breakdown of djerfisherite (Djr) in Y-691. Along with secondary troilite (Tr), idaite-bornite crystals (Id) were formed.

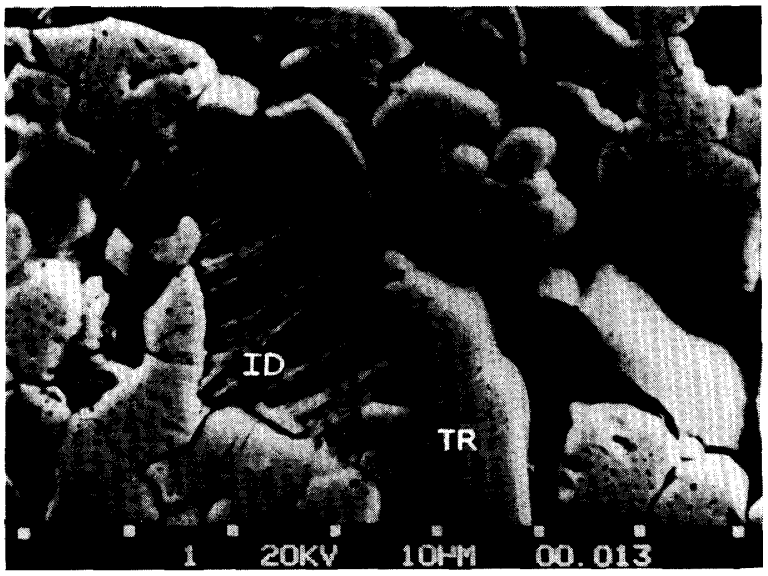

Fig. 17. A high magnification SEM image of idaite (Id) with well developed basal cleavage surrounded by secondary troilite in Y-691. Both minerals were formed by the Qingzhen Reaction.

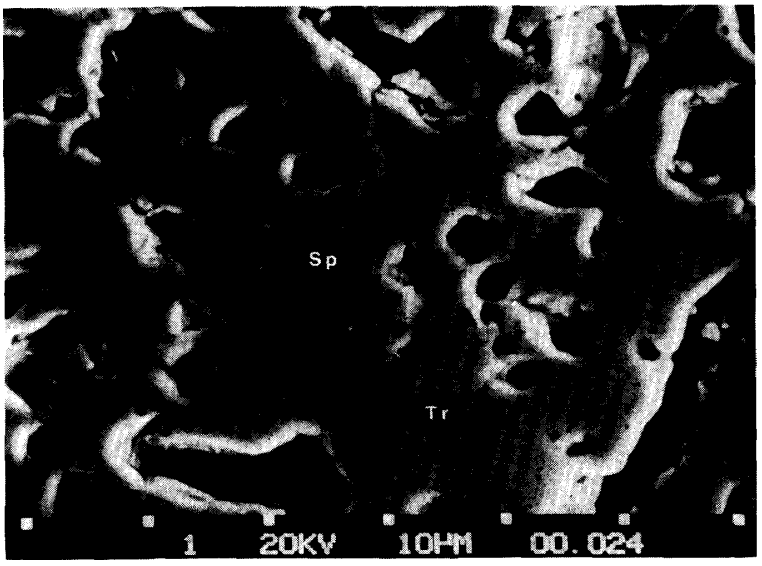

Fig. 18. SEM photograph of secondary sphalerite (Sp) formed with secondary troilite (Tr) by the Qingzhen Reaction in Y-691. Both minerals display the same spongy appearance due to the presence of bubbles.

not contain any detectable Zn. Figure 18 is a SEM closeup of the troilite-sphalerite intergrowth. It indicates that sphalerite is porous as well. This is strong evidence for simultaneous formation of sphalerite and secondary troilite. This breakdown texture indicates a thermal episode to which both Qingzhen and Y-691 were subjected after their solidification.

6. Mineral Chemistry

Evaluation of the chemical compositions of the mineral constituents of Qingzhen and Y-691 revealed resolvable systematic differences. This is remarkable in view of the fact that both meteorites are highly unequilibrated EH3s. Study of these diffferences enabled, for the first time, a better understanding of the evolution of the EH chondrites. Planetary metamorphic events have been recognized and the conditions during these episodes have been estimated (EHLERS and EL GORESY, 1988; EL GORESY and EHLERS, 1988).

6.1. Silicates

One of the most remarkable features is the depletion of potassium in chondrules. The bulk of djerfisherite is confined to the clasts and veins in the matrix. The glass in the chondrules is usually Na-rich and depleted in K (Table 5). Compositions of the glass are quite variable and the SiO_2 content ranges between 56.0 and 96.0 wt% (Fig. 19). The Al_2O_3 contents also vary widely between 0.4 and 29.7 wt%. Results of 26 analyses revealed an excellent correlation between SiO_2 and Al_2O_3 contents (Fig. 19). The glasses are enriched in both Na and Cl. The calculated Na/K ratios are usually high with only one exception. The measured ratio vary between 20 and 101 with the majority clustering between 20 and 60 (Fig. 19). The Cl content is also highly variable. It is lowest in the SiO_2-rich members. The highest concentration encountered is 4.4 wt%. One would expect these glasses to be enriched in I; hence they are good

Table 5. Examples of glass compositions in chondrules from Qingzhen.

Element	1	2	3	4	5
CaO	0.02	0.04	0.11	n.d.	n.d.
MgO	0.06	4.26	8.20	2.45	2.43
Na_2O	4.27	3.95	2.62	5.46	0.55
K_2O	0.07	0.17	0.07	0.05	0.02
FeO	0.18	0.29	0.52	0.13	0.13
MnO	0.02	0.04	0.09	0.02	n.d.
TiO_2	0.15	0.06	0.11	0.03	0.19
V_2O_3	n.d.*	n.d.	n.d.	n.d.	n.d.
Cr_2O_3	0.06	0.31	0.11	0.02	0.16
Al_2O_3	27.4	15.4	11.2	14.0	1.93
SiO_2	63.0	73.1	75.2	78.7	91.4
Cl	4.27	0.44	0.09	n.d.	0.10
Total	99.50	98.06	98.32	100.86	96.91

* n.d.=not detected.

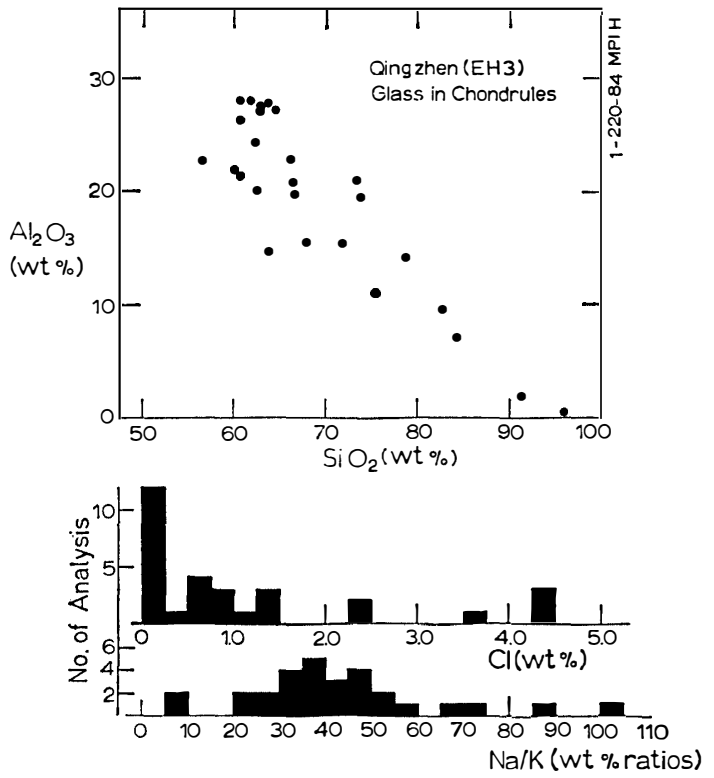

Fig. 19. *SiO_2 vs. Al_2O_3 contents of glass in the chondrules of Qingzhen. The lower part of the diagram depicts the Cl-contents of the glass and the Na/K ratios.*

candidates for ^{129}I-^{129}X studies. Enstatite analyses were conducted only for Qingzhen. The results indicate a narrow range of composition with FeO contents from 0 to 3 wt% *i.e.* 0 to 4 mole% Fs (EL GORESY *et al.*, 1983). High-Fe relict grains in the cores of pure enstatite were reported by KITAMURA *et al.* (1986) and LUSBY *et al.* (1987).

6.2. *Metals and sulfides*

6.2.1. Kamacite

Compositions of kamacites in Qingzhen are distinct from those in Y-691. Kamacites in both meteorites clearly differ in their Si-content. In Qingzhen Si varies between 2.25 and 3.0 wt% whereas in Y-691 Si ranges from 1.4 to 2.4 wt%. This difference is well-resolved (Fig. 20), indicating that Qingzhen was formed under slightly more reducing conditions than Y-691. The Ni content in kamacite in both meteorites is very similar and varies between 1.5 and 4.0 wt% (Fig. 20). In BSE imaging a polycrystalline intergrowth between dark and bright metal phases was recognized. Electron probe analyses of both phases revealed no measurable compositional differences. We suspect that they are kamacite (dark) and taenite (bright) with similar chemical compositions. Co is highly fractionated in kamacite; concentrations vary between 0.25 and 0.35 wt%. In both meteorites the coexisting perryite does not contain any detectable Co.

6.2.2. Perryite

A compositional dichotomy is also encountered in perryite. Although the Si contents of perryite in both meteorites are comparable (11.8–13.0 wt%), the Ni contents are different and the analyses points cluster in two separate fields (Fig. 21). The Ni-content of perryite in Qingzhen is higher than in Y-691. The Fe/Ni ratios of both meteorites are very similar: 15.5 for Qingzhen (this work) and 16.4 for Y-691 (KALLEMEYN and WASSON, 1986). Figures 20 and 21 indicate that the dichotomy in kamacite and perryite compositions is genetically interrelated. Perryites in both meteorites also contain fair amount of Cu (0.27–0.42 wt%). Thus Cu partitions between djerfisherite and perryite.

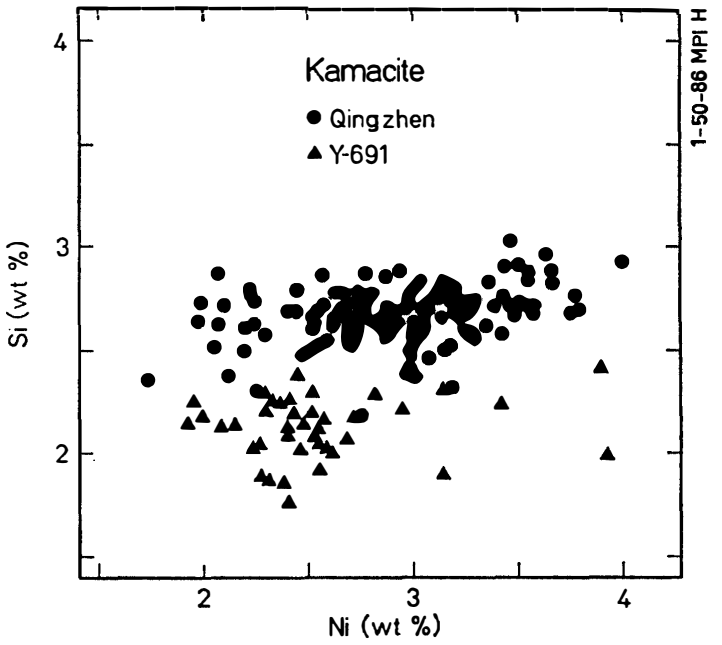

Fig. 20. Si and Ni concentrations of kamacites in Qingzhen and Y-691.

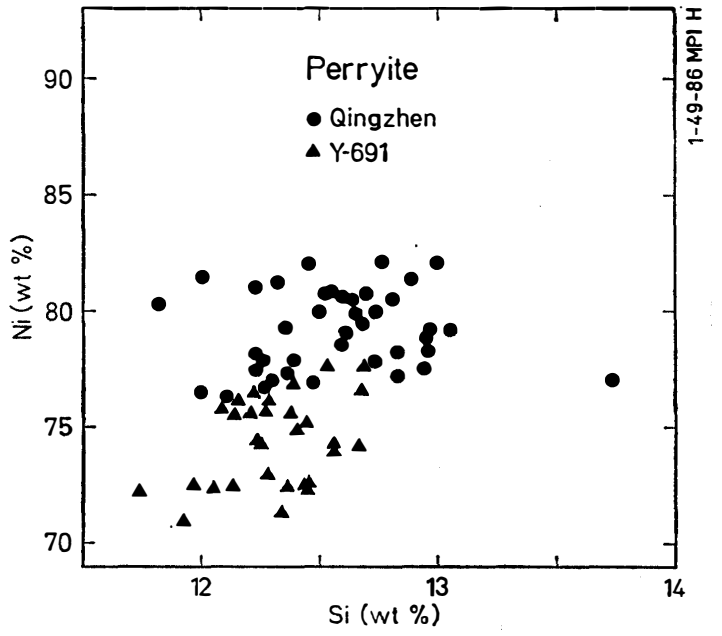

Fig. 21. Ni vs. Si-contents of perryite in Qingzhen and Y-691. Perryite in Y-691 contains less Ni than Qingzhen.

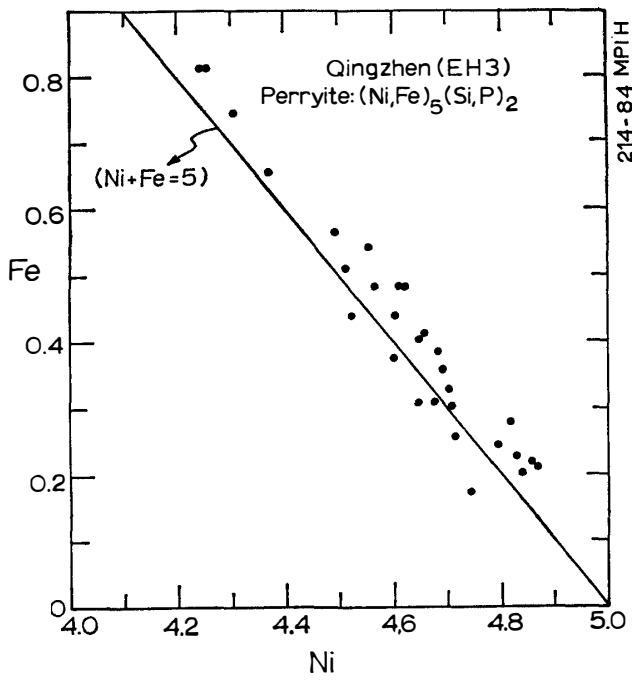

Fig. 22. Fe vs. Ni cations in perryite in Qingzhen. The points cluster along the stoichiometric line.

In contrast, coexisting kamacite does not contain any detectable Cu. All measured perryite compositions (more than 70 analyses) satisfy the stoichiometric composition with an (Ni+Fe) : (Si+P) ratio close to 5 : 2. The Ni : Fe ratios are indicative of substitutional behavior (Fig. 22).

6.2.3. Schreibersite

Composition of schreibersite in Qingzhen and Y-691 is indistinguishable from each other. They fall in the same narrow range with Ni-contents between 13.1 and 15.7 wt% (Table 6). Schreibersite in both meteorites was found to contain measurable amounts of Si (0.14–0.35 wt%). Thus, Si is not confined only to perryite and kamacite. The schreibersite spherules in oldhamite and niningerite were unfortunately too small to analyze quantitatively.

Table 6. Composition of schreibersite in Qingzhen and Y-691 selected from 45 analyses (in wt%).

Element	1	2	3	4	5	6
	(Qingzhen)			(Y-691)		
Fe	69.3	70.1	71.8	68.3	70.0	71.2
Ni	15.7	15.5	12.5	15.6	14.4	13.1
Co	n.d.*	n.d.	n.d.	n.d.	n.d.	n.d.
Cu	n.d.	n.d.	n.d.	n.d.	n.d.	n.d.
Cr	n.d.	n.d.	0.33	n.d.	n.d.	n.d.
Si	0.25	0.26	0.16	0.14	0.14	0.16
P	15.1	15.1	15.0	14.2	13.9	13.6
Total	100.35	100.96	99.79	98.24	98.44	98.06

* n.d.=not detected.

6.2.4. Niningerite

Niningerite compositions in the EH group cluster in three distinct subgroups in the MgS-FeS-MnS compositional diagram (Fig. 23): (a) a subgroup with the lowest MnS content (3.6–6.7 mole%) and the highest MgS content (73.2–82.9 mole%) comprising Y-691, (b) a subgroup with medium MnS (7.5 mole%) and lowest MgS contents (58.0–65.5 mole%) comprising Indarch, and (c) a subgroup with high MnS content (12–14 mole%) and medium MgS contents (61–75 mole%) consisting of Y-74370, Qingzhen, Kota Kota, Kaidun III, and St. Marks. The three subgroups are arranged in three distinct fields, all lying parallel to the MgS-FeS join (Fig. 23). This indicates that the MnS content is the key genetic component in the evolution of the niningerite-bearing assemblages in EH chondrite. The Mn content of EH chondrites are very similar (KALLEMEYN and WASSON, 1986). Consequently, the observed differences in the MnS contents of niningerites are indicative of different partitioning of Mn between niningerite and enstatite as a function of f_{S2}. High f_{S2} would lead to high MnS contents in niningerites and *vice versa*. Furthermore, variation in the FeS and MgS contents in niningerites of the third subgroup reflects an evolution sequence; Y-74370 being the most primitive and Kaidun III and St. Marks the most equilibrated in this subgroup. More recent investigations included other EH chondrites like Abee, South Oman, and a reinvestigation of Y-74370 (EHLERS and EL GORESY, 1988). These studies revealed that Abee belongs to the first subgroup. The niningerites in this meteorite have the highest FeS content ever found in EH chondrites (EHLERS and EL GORESY, 1988). A systematic study of individual niningerite grains in Abee, South Oman, St. Marks, Kaidun III, Qingzhen, Y-691, Indarch, and Y-74370 revealed that niningerites in all EHs are zoned (EHLERS and EL GORESY, 1988). A normal zoning trend with decreasing FeS content from the cores to the rims adjacent to the neighboring troilite was encountered in Abee, South Oman, St. Marks, Kaidun III, and Y-74370. In

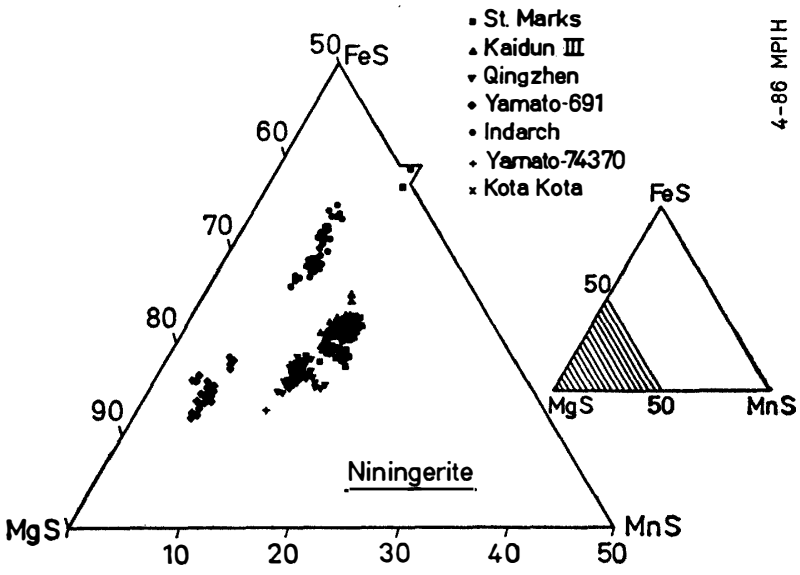

Fig. 23. Compositions of niningerites in EH chondrites in the MgS-FeS-MnS compositional diagram.

contrast, a reverse trend with increasing FeS content from core to rim was found in niningerites in Y-691, Indarch, and Qingzhen. EHLERS and EL GORESY (1988) interpret the latter trend as a result of thermal episodes in the EH parent body which leads to Fe diffusion from troilite to the neighboring niningerite. The Ca content of niningerites in Qingzhen and Y-691 is very low and varies between 0.34 and 0.47 wt%. In addition, few niningerite grains coexisting with djerfisherite in Y-691 were found to contain minor concentrations of Cu ranging between 0.02 and 1.3 wt% (Table 7).

Table 7. Examples of Cu-bearing niningerite in Y-691.

Element	1	2	3	1	2	3
Mg	32.1	32.0	31.6	0.833	0.818	0.813
Fe	14.0	14.2	14.0	0.158	0.157	0.156
Mn	4.00	3.57	3.90	0.046	0.040	0.045
Ca	0.46	0.49	0.38	0.007	0.007	0.006
Cr	0.11	0.14	0.16	0.002	0.002	0.002
Cu	0.48	1.30	0.020	0.005	0.013	0.020
S	48.3	49.7	49.1	0.950	0.962	0.958
Total	99.5	101.4	101.14	2.001	1.999	2.016

Table 8. Compositions of oldhamite in Qingzhen and Y-691 selected out of 70 analyses (in wt%).

Element	1	2	3	4	5	6
	Qingzhen			Y-691		
Ca	54.4	54.8	52.9	54.3	53.5	54.0
Fe	0.08	0.81	1.70	0.68	0.63	0.59
Mn	0.20	0.13	0.16	0.09	0.09	0.06
Mg	0.46	0.47	0.58	0.41	0.39	0.39
Zn	0.07	0.03	n.d.	0.14	0.12	0.12
Cu	n.d.	0.03	n.d.	0.18	0.21	0.18
Ni	n.d.	n.d.	0.14	0.10	0.10	0.09
Co	n.d.	0.03	n.d.	n.d.	n.d.	n.d.
Cr	n.d.	n.d.	n.d.	0.04	n.d.	n.d.
S	43.7	45.0	42.7	43.3	42.8	43.3
Total	98.91	101.3	98.18	99.24	97.84	98.73
Ca	0.988	0.973	0.973	0.988	0.988	0.986
Fe	0.000	0.012	0.023	0.009	0.008	0.008
Mn	0.004	0.000	0.004	0.001	0.001	0.001
Mg	0.016	0.016	0.020	0.013	0.012	0.012
Zn	0.000	0.000	0.000	0.002	0.001	0.001
Cu	0.000	0.000	0.000	0.002	0.002	0.002
Ni	0.000	0.000	0.000	0.001	0.001	0.001
Co	0.000	0.000	0.000	0.000	0.000	0.000
Cr	0.000	0.000	0.000	0.000	0.000	0.000
S	0.992	1.000	0.984	0.984	0.986	0.989

6.2.5. Oldhamite

Compositions of oldhamites in Qingzhen and Y-691 are quite uniform. They are usually low in Fe (0.08–1.70 wt%), Mn (0.06–0.16 wt%), and Mg (0.39–0.58 wt%). Examples of oldhamite compositions are given in Table 8.

6.2.6. Troilite

Generally, the compositions of troilites in both meteorites are similar. The metal/sulfur ratios are usually close to 1 indicating that they are stoichiometric. There are, however, differences between compositions of primary and secondary troilites, on the one hand, and between primary troilites in Qingzhen and Y-691 on the other. Chromium contents of primary troilites are variable and appear to depend on the amount of microscopic and submicroscopic daubreelite lamellae. In both meteorites the Cr content varies between 0.70 and 2.04 wt%. Ti-content of primary troilite is usually lower than 0.35% and hence is lower than the contents in other EH chondrites. Troilites in Qingzhen are systematically lower in Ti than in Y-691 (0.10–0.19% *vs.* 0.20–0.33%, respectively). Activity of FeS in primary troilite always deviates from unity and varies between 0.97 and 0.98. Compositions of secondary troilite differ distinctly from that of primary troilite in two aspects. Secondary troilite does not contain any detectable Ti. Cr-contents are also lower than in primary troilite (Table 9). Secondary troilites also contain minor amounts of Cl (0.15–0.44%). It is unclear if Cl is present in the troilite structure, or in fine-grained interstitial material. In addition the FeS activity in secondary troilite is usually close to unity (Table 9). This is remarkable in view of the application of the sphalerite cosmobarometer for estimation of the total pressures during the metamorphic episodes in the EH chondrites.

Table 9. Composition of primary and secondary troilites in Y-691.

Element	1	2	3	4	5	6
	Primary troilite			Secondary troilite		
Fe	61.6	61.0	62.1	63.4	63.7	61.7
Cr	0.91	1.04	1.13	0.52	0.45	0.42
Ti	0.32	0.20	0.21	n.d.	n.d.	n.d.
S	36.8	36.4	36.9	35.3	35.4	34.8
Cl	n.d.	n.d.	n.d.	0.15	0.20	0.44
Ca	n.d.	n.d.	n.d.	0.10	0.06	0.09
Total	99.63	98.64	100.34	99.47	99.81	97.45
	Number of atoms per formula unit					
Fe	0.970	0.970	0.972	1.008	1.008	1.000
Cr	0.016	0.018	0.019	0.008	0.008	0.008
Ti	0.006	0.004	0.004	0.000	0.000	0.000
S	1.009	1.009	1.006	0.977	0.977	0.980
Cl	0.000	0.000	0.000	0.004	0.004	0.012
Ca	0.000	0.000	0.000	0.004	0.000	0.004
Total	2.001	2.001	2.001	2.001	1.997	2.004

6.2.7. Daubreelite

Daubreelite grains in Y-691 were unfortunately too small to be successfully analyzed. NAGAHARA (1985) reported 2.5 wt% Zn. Our analyses of daubreelites in Qingzhen revealed that: (1) All daubreelites contain considerable amounts of Na ranging between 0.20 and 0.45 wt%. This is the first report of Na in a spinel-type mineral in meteorites. (2) Daubreelites in Qingzhen contain the highest Zn content ever found in EH chondrites. Zn-concentrations vary between 5.70 and 8.11 wt% (Table 10).

Table 10. Composition of zincian daubreelites in Qingzhen selected out of 36 analyses (in wt%).

Element	1	2	3	4	1	2	3	4
					Number of ions per formula unit			
Fe	13.3	12.2	11.4	11.1	0.703	0.633	0.602	0.570
Zn	5.70	6.61	7.53	8.11	0.258	0.293	0.340	0.355
Cu	0.23	n.d.	0.23	0.19	0.012	0.000	0.012	0.008
Mn	0.52	0.89	0.46	0.32	0.027	0.047	0.023	0.016
Ca	n.d.	n.d.	n.d.	n.d.	0.000	0.000	0.000	0.000
Cr	35.5	36.0	35.5	35.6	2.008	2.000	2.008	1.965
Ti	n.d.	0.09	0.05	0.10	0.000	0.004	0.004	0.004
Na	0.34	0.24	0.39	0.32	0.043	0.031	0.051	0.039
S	43.0	44.2	43.2	45.1	3.949	3.984	3.965	4.031
Metal sulfur ratios					0.773	0.755	0.767	0.734
Total	98.59	100.23	98.76	100.84				

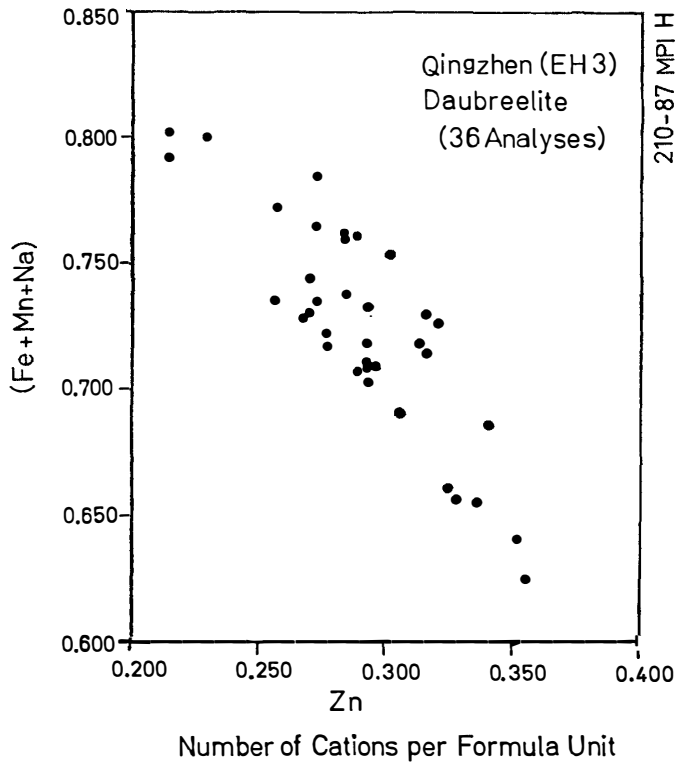

Fig. 24. (Fe+Mn+Na) cations vs. Zn cations of daubreelite in Qingzhen.

Metal/sulfur ratios vary between 0.734 and 0.773, thus indicating a very small deviation from stoichiometry. Zn is very probably substituting for Fe in the tetrahedral site. A plot of Zn *vs.* (Fe+Mn+Na) indicates a linear correlation with the points clustering around the stoichiometric ratio (Fig. 24). Several points, however, lie above the stoichiometric ratio.

6.2.8. Djerfisherite

Djerfisherite abundance in EH chondrites does not appear to follow a distinct

Table 11. Compositions of djerfisherite in Qingzhen and Y-691 selected from 56 analyses (in wt%).

Element	1†	2†	3*	4*
K	8.08	8.40	7.07	7.94
Na	0.92	0.70	1.52	1.14
Ca	n.d.	n.d.	0.01	n.d.
Fe	53.5	54.5	51. 6	50.9
Cu	3.16	2.31	2.62	4.73
Ni	1.35	1.32	3.02	0.49
Zn	n.d.	n.d.	n.d.	n.d.
Mn	0.03	n.d.	0.13	0.01
Cr	n.d.	n.d.	0.04	0.04
S	30.3	29.6	31.2	32.2
Cl	1.48	1.48	1.49	1.50
Total	98.82	98.31	98.70	98.95

† Analyses from Qingzhen.

* Depicting two distinct djerfisherite types in Y-691.

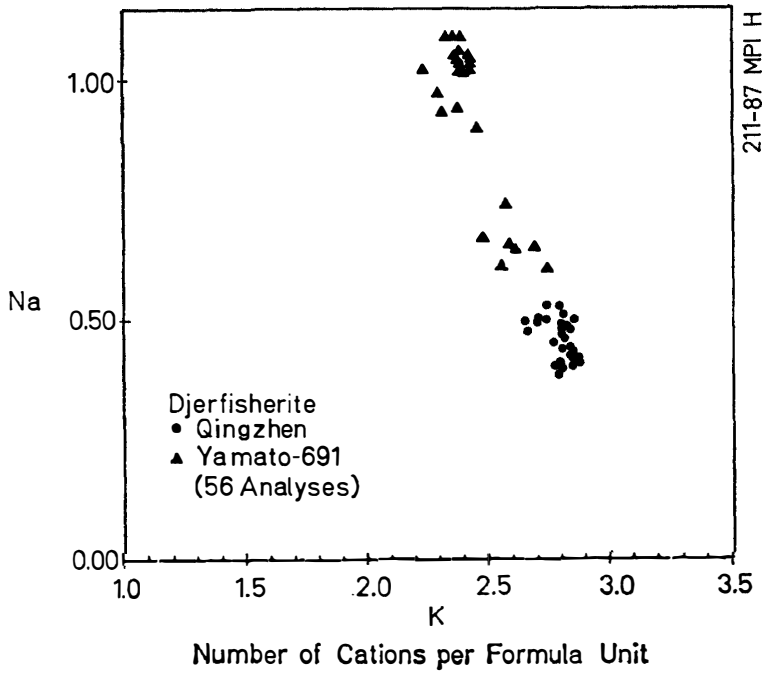

Fig. 25. Na cations vs. K cations in djerfisherite in Qingzhen and Y-691.

pattern. The mineral is abundant in Qingzhen, less abundant in Y-691, sporadic in St. Marks, and very rare in Kaidun III and Y-73470. It appears to be absent in Indarch, Abee, South Oman, and Kota Kota. In Y-691 two distinct djerfisherite varieties were

Table 12. Composition of caswellsilverite in Qingzhen selected from 25 analyses (in wt%).

Element	1	2	3	1	2	3
				Number of ions per formula unit		
Na	15.8	15.7	15.9	0.949	0.953	0.953
K	n.d.	n.d.	n.d.	0.000	0.000	0.000
Cu	n.d.	n.d.	n.d.	0.000	0.000	0.000
Zn	n.d.	n.d.	n.d.	0.000	0.000	0.000
Ca	0.17	0.20	n.d.	0.004	0.008	0.000
Fe	0.85	0.72	0.77	0.020	0.020	0.020
Mn	0.11	0.08	n.d.	0.004	0.004	0.000
Cr	37.5	37.0	37.5	0.996	0.992	0.996
Ga	n.d.	n.d.	n.d.	0.000	0.000	0.000
S	46.9	46.6	46.9	2.023	2.027	2.027
Total	101.33	100.3	101.07			

Table 13. Composition of new Na-Ca-Cr-sulfide in Y-691.

Element	1	2	3	4	5	6
Na	15.7	14.6	13.6	10.6	8.86	4.95
K	0.01	n.d.	0.02	0.10	0.06	0.10
Cu	1.29	2.23	3.95	5.19	9.48	14.7
Zn	n.d.	0.23	0.55	0.03	0.19	0.40
Ca	n.d.	n.d.	n.d.	0.03	0.01	n.d.
Fe	1.06	0.76	1.83	1.04	2.00	1.70
Mn	0.05	0.09	0.09	0.05	0.07	0.05
Cr	37.3	37.2	36.2	36.6	35.0	33.9
Ga	n.d.	n.d.	n.d.	n.d.	n.d.	n.d.
S	44.4	44.3	43.8	44.5	44.0	42.8
Total	99.81	99.41	99.49	98.14	99.67	98.60
			Number of cations per formula unit			
Na	0.962	0.912	0.857	0.696	0.586	0.348
K	0.000	0.000	0.004	0.016	0.000	0.004
Cu	0.030	0.051	0.090	0.122	0.227	0.375
Zn	0.000	0.005	0.012	0.004	0.004	0.012
Ca	0.000	0.000	0.000	0.004	0.000	0.000
Fe	0.024	0.019	0.048	0.028	0.055	0.051
Mn	0.002	0.003	0.003	0.001	0.000	0.000
Cr	1.019	1.035	1.010	1.060	1.027	1.055
Ga	0.000	0.000	0.000	0.000	0.000	0.000
S	1.962	1.984	1.981	2.090	2.094	2.156
Total	3.999	4.009	4.005	4.021	3.993	4.001
Cation/anion ratio	1.038	1.021	1.022	0.924	0.907	0.856

encountered: (a) A variety high in Cu (4.73 wt%), low in Ni (0.49 wt%), and low in Na (1.14 wt%), and (b) a variety moderate in Cu (2.26 wt%), high in Ni (3.02 wt%), and high in Na (1.52 wt%). The second variety contains somewhat less K than the first (Table 11). In comparison, compositions of djerfisherite in Qingzhen have a narrow range and are well separated from those in Y-691 (Fig. 25). In addition, Fig. 25 depicts

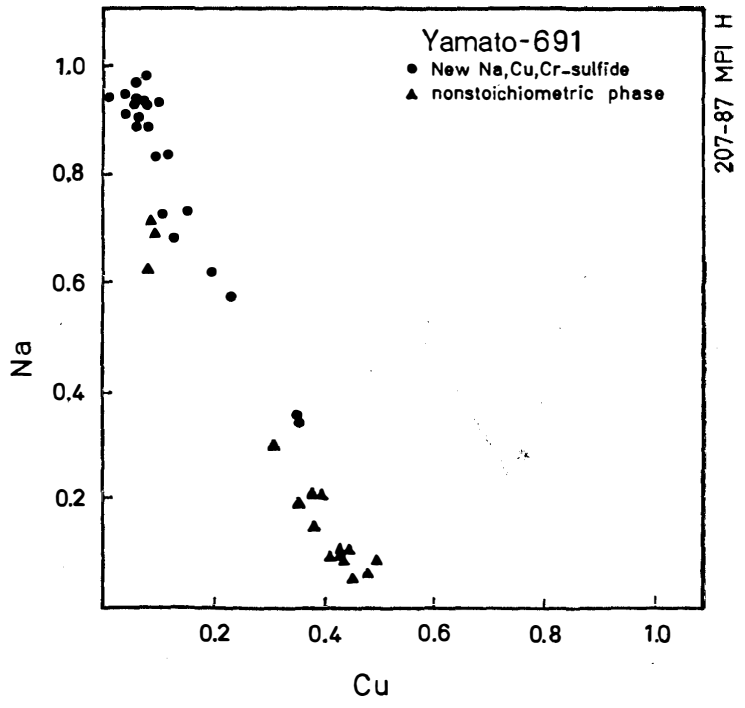

Fig. 26. Na cations vs. Cu cations in new Na-Cu-Cr-sulfide (circles) and Na-Cu-Zn-Cr-sulfide (nonstoichiometric phase).

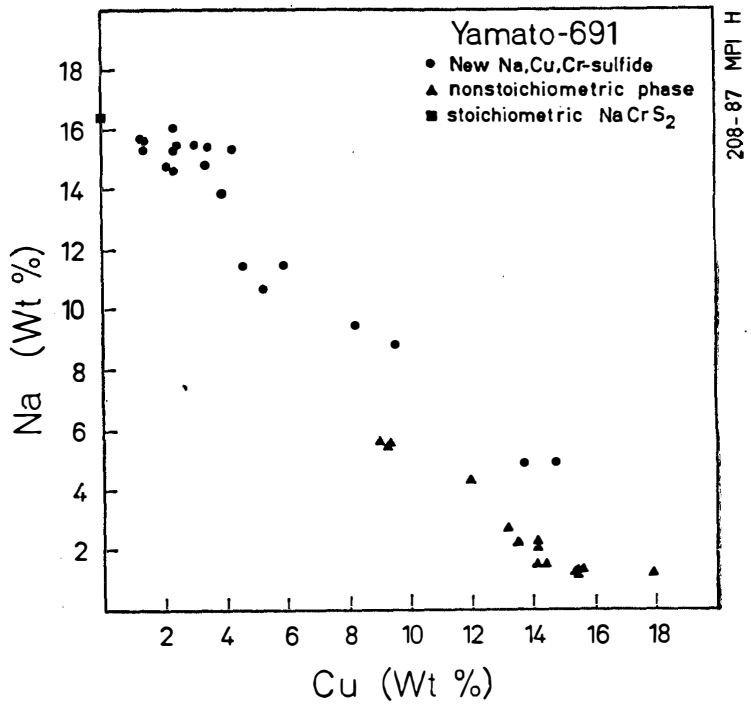

Fig. 27. Na and Cu concentrations in the new Na-Cu-Cr-sulfide (circles) and Na-Cu-Zn-Cr-sulfide (nonstoichiometric phase).

the bimodal distribution in the djerfisherite compositions in Y-691. The variations in djerfisherite compositions in Y-691 reflect very probably the low degree of equilibration of this meteorite.

6.2.9. Caswellsilverite and related phases

This mineral is quite rare in Y-691. Instead a new Cu-bearing variety was encountered. In Qingzhen caswellsilverite is almost a pure Na-Cr-sulfide. It contains very small amounts Ca, Fe, and Mn. No K was detected in any of the 25 grains analyzed.

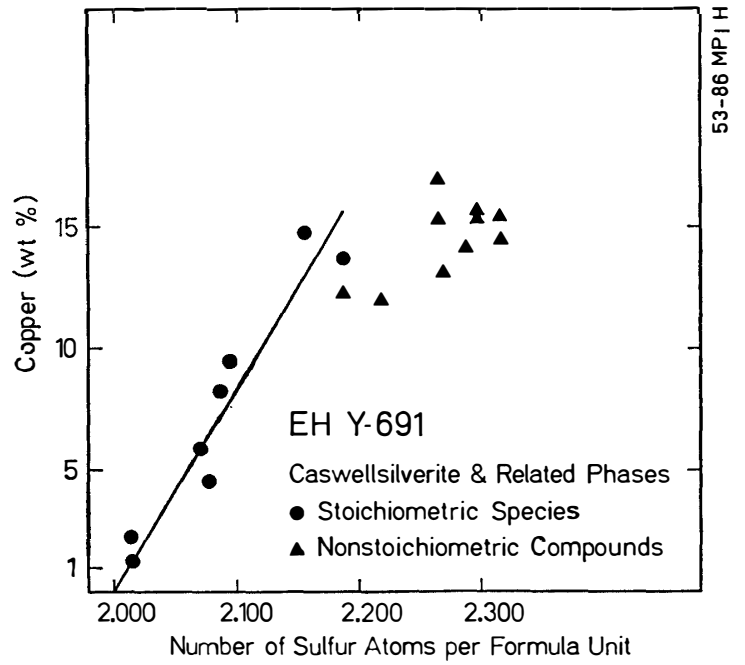

Fig. 28. Cu concentration vs. number of sulfur atoms in the new Na-Cu-Cr-sulfide and Na-Cu-Zn-Cr-sulfide (nonstoichiometric compounds).

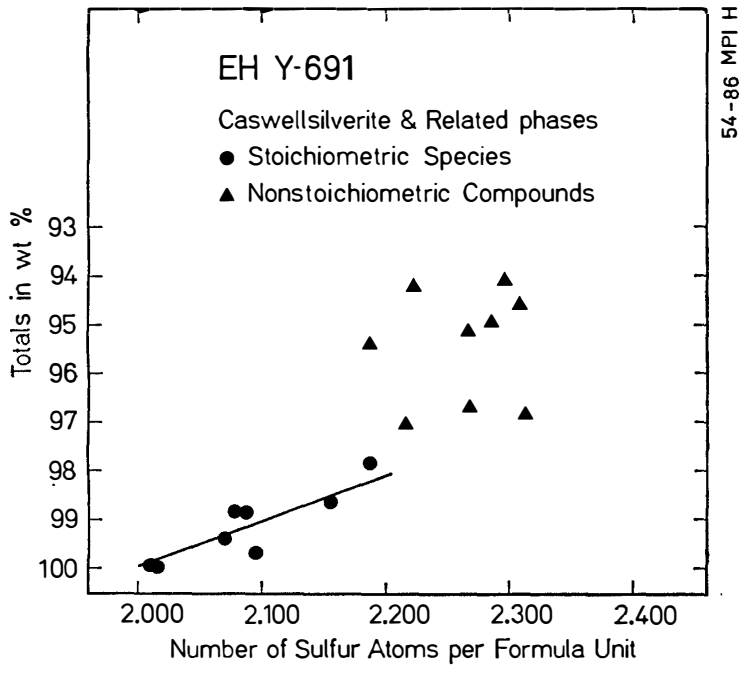

Fig. 29. Analysis totals vs. number of sulfur atoms in the new Na-Cu-Cr-sulfide and Na-Cu-Cr-sulfide (nonstoichiometric compounds).

Examples of caswellsilverite compositions in Qingzhen are given in Table 12. The mineral is usually a stoichiometric $NaCrS_2$ (Table 12).

Compositions of the brownish, strongly pleochroic mineral in Y-691 indicate that it is related to caswellsilverite. The mineral contains variable amounts of Cu, presumably substituting for Na (Table 13). The lowest Cu contents (1.29 wt%) occur in the Na-rich members (analysis # 1, Table 13) and *vice versa* (analysis # 6 in Table 13, 14.7 wt% Cu, 4.95 wt% Na). This is also shown in Figs. 26 and 27. The chemical formula resembles that of caswellsilverite and can be written: (NaCu) CrS_2. Table 13 also indicates that the metal/sulfur ratio decreases with increasing Cu content (Fig. 28). Analysis totals for the Cu-rich members are also lower than the Cu-poor ones (Fig. 29).

6.2.10. Hydrated Na-Cr-sulfides

There are three distinct types of hydrated sulfides:

(a) A Zn-rich variety found only in Y-691. This phase was formed presumably by the alteration of the brownish Cu-rich Na-Cr-sulfide during the metamorphic episode.

Table 14. Composition of new Na-Cu-Zn-Cr-sulfide in Y-691.

Element	1	2	3	4
Cr	34.1	33.34	33.9	32.5
Mn	0.10	0.09	0.05	0.03
Fe	0.73	4.71	1.14	0.65
Ca	0.05	0.09	0.08	0.76
Cu	5.04	4.62	6.99	7.62
Zn	6.49	5.96	8.52	9.97
Ga	n.d.	n.d.	n.d.	n.d.
K	0.06	0.20	0.17	0.30
Na	12.9	3.36	7.41	1.86
S	43.9	42.3	43.8	42.4
Total	103.36	94.67	102.06	96.06

Table 15. Examples of compositions of hydrated Na-Cr-sulfides in Qingzhen.

Element	1	2	3	4
	Phase A		Phase B	
Na	1.14	1.13	2.35	1.94
K	n.d.	n.d.	0.47	0.51
Ca	0.07	n.d.	0.82	0.20
Mg	n.d.	n.d.	n.d.	n.d.
Fe	0.63	0.72	1.36	0.28
Mn	n.d.	n.d.	n.d.	n.d.
Zn	n.d.	n.d.	n.d.	n.d.
Cu	n.d.	n.d.	n.d.	n.d.
Cr	39.0	39.6	30.6	31.7
Ti	0.08	0.04	n.d.	n.d.
S	51.9	51.5	35.5	36.8
Total	92.82	92.95	71.10	71.43

This compound contains variable amounts of Zn and Cu (6.49–9.97 wt% Zn and 4.62–7.62 wt% Cu) (Table 14).

(b) Mineral A, found only in Qingzhen. Analysis totals usually sum to values between 88 and 92 wt%. The mineral is very low in Na and does not contain K (Table 15). It also contains variable amounts of Fe (0.30–0.85 wt%). The Cr and S contents are usually higher than in caswellsilverite.

(c) Mineral B, also only found in Qingzhen, is characterized by much lower analysis totals than for mineral A (Table 15), between 70 and 76 wt%. In comparison to mineral A, it contains higher Na- but much lower K-content.

We suspect that the low totals are due to the presence of H_2O or OH. Compositions of mineral A and B are distinctly different from that of schoellhornite (OKADA *et al.*, 1985). The minerals may be however structurally related to it or other chalcogenides. Their characterization requires detailed analysis using TEM techniques.

6.2.11. Greigite and smythite

Several analyses indicated that the minerals are pure iron sulfides (Table 16). The atomic Fe/S ratio is 3.21 : 4 and is hence strnogly suggestive of greigite.

Table 16. Composition of greigite in Qingzhen.

Element		Number of cations per formula unit
Fe	56.9	3.211
Ni	0.06	0.004
Co	n.d.*	0.000
Cr	n.d.	0.000
Ti	n.d.	0.000
S	40.7	4.000
Total	97.66	

* n.d.=not detected.

6.2.12. Sphalerite

Chemistry of sphalerites in EH chondrites is very complex and reflects the complicated stages during the formation of EH chondrites in the nebula and in the parent bodies. In Qingzhen and Y-74370 an exotic Ga-rich variety was discovered (RAMBALDI *et al.*, 1986; NAGAHARA and EL GORESY, 1984). In Qingzhen Ga-rich sphalerite was encountered as inclusions in kamacite. It coexists with a Cu-Fe-sulfide, presumably a member of the Intermediate Solid Solution series in the Fe-Cu-S system (CABRI, 1973). Ga contents of the sphalerite range between 2.15 and 3.7 wt% (RAMBALDI *et al.*, 1986). The grains also contain considerable amounts of Cu (1.07–2.20 wt%). NAGAHARA and EL GORESY found in Y-74370 an identical assemblage. They reported a Ga content of 4.8 wt% in sphalerite.

In Qingzhen and Y-691, Ga-free sphalerite was encountered (EL GORESY, 1985; EL GORESY and EHLERS, 1988). In Y-691 two genetically and chemically distinct sphalerites occur: (a) coarse-grained primary sphalerite in sphalerite-troilite fragments. The grains are not zoned and have a very narrow range in their FeS contents (48–49 mole% FeS). (b) Fine-grained porous sphalerite associated with the djerfisherite break-

down assemblage. This type also displays a very narrow range in its FeS contents. The FeS-concentration is, however, distinctly lower than in the primary sphalerite (43 mole%).

In Qingzhen, sphalerite is chemically inhomogeneous in individual grains and from grain to grain. The measured compositional profiles are strongly suggestive of diffusion controlled Fe-concentration paths to the neighboring troilite. In the cores of the grains the FeS content also varies between 46 and 49 mole%. At the contact to troilite the FeS-content is 43 mole%. It is remarkable that (1) the composition of the sphalerite cores in Qingzhen is almost identical to the composition of primary sphalerite in Y-691, and (2) the composition of the sphalerite rims adjacent to troilite in Qingzhen is also identical to the composition of secondary sphalerite in Y-691. Chemistry and the genetic relations of sphalerite in connection with aspects of sphalerite barometry in EH chondrites will be treated in detail elsewhere (EL GORESY and EHLERS, 1988).

6.2.13. Idaite and bornite

These minerals are intimately intergrown, hence attempts to analyze the phases separately failed. Analysis of a composite grain consisting chiefly of idaite revealed: 19.1 wt% Fe, 48.0 wt% Cu, 0.12 wt% Zn, and 30.0 wt% S. This composition plots between idaite and bornite compositions in the Fe-Cu-S system.

7. Discussion

The results of the present investigations reveal the establishment of petrological trends and distinct systematics in mineral chemistries of EH chondrites. They reveal also information on variation of oxygen and sulfur fugacities, thermal histories, and planetary metamorphic events. We argue that these findings allow a construction of an evolution scheme of the EH chondrites in the solar nebula and in the parent bodies after accretion.

The relative abundance of sulfide and metal clasts is distinctly higher in EH3s *e.g.* Y-691, Y-74370, and Qingzhen, than in EH4s, St. Marks, Kaidun III, and Indarch. Metals and sulfides in the latter three EH4s occur usually as coarse-grained assemblages in the interstices of enstatite and other silicates. We argue that the metal sulfide clasts, fragments, and complex spherules in EH3s are individual entities preserving a considerable part of their primordial textures since their accretion with the matrix. Two important observations support this interpretation: (a) Niningerite and oldhamite, the highest temperature condensates (LARIMER and BARTHOLOMAY, 1979), occur in the interiors of the majority of the different clasts, fragments, and spherules indicating that the surrounding metals and sulfides accreted around them. The omnipresence of niningerite and oldhamite with the same textural signature in these objects is strongly suggestive of an intensive dust transport from the source regime of the mineral pair to the various regimes where the different clast types grew by condensation. (b) Niningerite and oldhamite usually occupy the cores of objects thus suggesting that the mineral pair acted as nuclei for accretion of the condensing metals and sulfides. The relative high abundance of niningerite in chondrules may also suggest that chondrule formation in EH chondrites took place prior to condensation of other sulfides like djerfisherite and daubreelite.

The behavior of Na and K in matrix and chondrules, however, cannot be explained by any current condensation model. Na and K are fractionated in two sulfide lithologies: (a) Na along with Cr in different sulfides, and (b) K with Fe, Ni, and Cu in djerfisherite. Na and Cr in EH chondrites are evidently coherent elements. Chondrules also contain a Na- and Cl-rich glass. It is however, remarkable that the chondrules are depleted in K whether or not Na is incorporated in glass, caswellsilverite, or both. The Na/K ratios of chondrules vary between 20 and 101. This indicates that the chalcophile behavior of the alkalies cannot be responsible for the K-depletion in the chondrules. From this evidence we can conclude that chondrules were formed by melting of preexisting grains originally depleted in K but enriched in Na and Cl. The fine texture stratigraphy of the metal-sulfide clasts indicate, however, that djerfisherite condensed after oldhamite, niningerite, and caswellsilverite and definitely *after* the chondrule formation. Unfortunately, there is no available thermodynamic data for caswellsilverite and djerfisherite to develop a quantitative condensation scheme for these sulfides.

The bimodal distribution in the compositions of djerfisherite is a further bench mark in resolving the evolution conditions of the EH chondrites. The bulk Na contents of Qingzhen and Y-691 are very similar (5980 and 5700 ppm respectively, KALLEMEYN and WASSON, 1986). The Na/K ratio in Qingzhen is, however, higher than in Y-691 (14 *vs.* 8.7). Hence the Na depletion of the Qingzhen djerfisherite have probably resulted during equilibration processes. Consequently, Y-691 should reveal evidence for less equilibration than Qingzhen. In fact the variation in the Na-contents of Y-691 djerfisherite and the presence of two djerfisherite types are strong arguments for a lower degree of equilibration. Another alternative to explain this dichotomy in Qingzhen and Y-691 is that the relatively higher f_{S2} and lower f_{O2} during the formation of Qingzhen may have favored a Na-depletion in djerfisherite. Unfortunately, we cannot further explore this possibility since the effect of f_{S2} and f_{O2} on the fractionation of alkalies among coexisting sulfides is not known.

Chemistry of niningerites establishes this mineral as a sensitive geochemical probe and an indicator for the thermal histories of EH chondrites. The MnS contents of niningerite resolve the EH chondrites into three distinct subgroups (Fig. 23). However, the Mn-contents of EH chondrites are comparable (KALLEMEYN and WASSON, 1986). Consequently, f_{S2} was the key factor for the partitioning of Mn between niningerite and the coexisting enstatite. The third subgroup (Y-74370, South Oman, Qingzhen, Kota Kota, Kaidun III, and St. Marks) must have formed in solar nebula regimes at *higher* f_{S2} than where Indarch and specifically Y-691 were condensed. On the other hand, the higher Si content in kamacite in Qingzhen in comparison to Y-691 (Fig. 20) is strongly suggestive that it also formed under *lower* f_{O2}. One can then conclude that there was a noticeable variations both in f_{S2} and f_{O2} in the part of the solar nebula where enstatite chondrites condensed. This would call for a chemical inhomogeneity and fractionation processes even in small regions of the nebula.

Zoning of niningerite reveals additional important information on the cooling rates of EH chondrites and the thermal episodes to which some members were subjected. Normal zoning is indicative of Fe diffusion from niningerite to troilite due to cooling in the nebula or in the EH parent body (EHLERS and EL GORESY, 1988). Estimation

of the cooling rates could then be achieved through quantitative evaluation of the Fe diffusion curves in niningerite and application of experimentally determined diffusion parameters (EHLERS, in preparation, 1988). Reverse zoning is straightforward evidence for diffusion of Fe from troilite to niningerite as a result of heating events (EHLERS and EL GORESY, 1988). Reverse zoning was encountered in Y-691, Indarch, and Qingzhen. These meteorites have low ^{40}Ar-^{39}Ar ages (MÜLLER and JESSBERGER, 1985; HONDA *et al.*, 1983). The *Qingzhen Reaction* in Y-691 and Qingzhen is additional ample evidence that these events took place in the parent body (EL GORESY, 1985). The lack of shock features in these two meteorites is strongly suggestive of endogenic processes. At least one difficulty arises from this interpretation. Young endogenic episodes (*e.g.* 800 Ma for Y-691 and 1.4 Ba for Qingzhen) would require a large parent body to provide long-lasting thermal activity. The textures in Qingzhen and Y-691 are not indicative of formation under high pressures. Recent investigations on Indarch indicate that this meteorite was subjected to at least two thermal events (EL GORESY and EHLERS, 1988).

The Qingzhen Reaction invokes breakdown of djerfisherite to secondary troilite and other secondary phases. In Y-691 secondary sphalerite, covellite, and idaite were formed during this reaction. The upper stability limit of covellite and idaite are 774 K and 780 K respectively. Consequently, the metamorphic event experienced by this meteorite must have taken place below 780 K. The compositional difference between the primary and secondary sphalerites in Y-691 (49 mole% FeS *vs.* 43 mole% FeS) indicates that secondary sphalerite was formed below the closure temperature of the primary sphalerite (EL GORESY and EHLERS, 1988). The presence of Fe diffusion profiles in sphalerite in Qingzhen, however, indicates that the metamorphic event in this meteorite took place above the sphalerite closure temperature (EL GORESY and EHLERS, 1988). This problem will be treated in detail in a separate report (EL GORESY and EHLERS, 1988).

There is an excellent inverse correlation between the relative abundance of the metal and sulfide clasts and the FeS-contents in niningerites in the third subgroup. This observation also holds true for Indarch and Y-691. We interpret this correlation as indicative of an evolution trend. Y-691 and Y-74370 are the least equilibrated in their subgroups, Indarch and St. Marks the highest in theirs (second and third). This interpretation is also in agreement with conclusions drawn by KEIL (1968). Our scheme, however, allows a much finer geochemical and petrological resolution within the EH chondrite family.

Zinc is a very important element in EH chondrites in view of its chalcophile behavior (KEIL, 1968; EL GORESY, 1985). It is partitioned between sphalerite and daubreelite. The total Zn contents in the studied EH chondrites vary between 74 and 300 ppm (KALLEMEYN and WASSON, 1986; this study). Apparently there is no correlation between the Zn content of a meteorite and the Zn-content of daubreelite. The highest Zn-contents in daubreelite (5.70–8.11 wt%) were found in Qingzhen. NAGAHARA (1985) reports 2.5 wt% Zn in daubreelite in Y-691, although the bulk Zn-content of this meteorite is higher than in Qingzhen (221 ppm *vs.* 184 ppm respectively). In Y-74370 NAGAHARA and EL GORESY (1984) report a concentration of 2.5 wt%. The total Zn content of this meteorite is comparable to that of Qingzhen (KALLEMEYN and

WASSON, 1986). KEIL's values for Kota Kota (5.2 wt%) are quite comparable to the values reported here for Qingzhen. BOCTOR and EL GORESY (1986) report Zn contents in daubreelite in St. Marks between 1.2 and 5.2 wt%. Considerable amounts of Zn could be incorporated in daubreelite formed by the invariant reaction $2CrS+2FeS \rightleftharpoons FeCr_2S_4+\alpha Fe$ only if sphalerite did not condense before formation of daubreelite. This invariant reaction takes place at 923 K (EL GORESY and KULLERUD, 1969). However, if sphalerite has condensed before formation of daubreelite, only a little Zn will be left to be incorporated in daubreelite. The lower Zn values measured in Y-691 and Y-74370 may support the latter possibility. However, these two measurements need to be confirmed before any further genetic interpretation can be made. A systematic study of the Zn-content of daubreelites is required for a better understanding of the behavior of this element during the formation of the EH chondrites.

Mobilization of Zn (and probably other volatile elements) during metamorphic events is established by the present investigations which revealed: (a) formation of secondary sphalerite and (b) formation of reaction rims of Na-Cu-Zn-Cr-sulfide around the Cu-bearing caswellsilverite. The source of the mobilized Zn is unknown. Primary sphalerite, and/or zincian daubreelite may have been the source material for the mobilized Zn. However we did not observe any evidence of breakdown or dissolution of either phase in any meteorite.

The two graphite forms in EH chondrites must have resulted from different formational processes. Graphite spherulites are encountered in low Ni and low Si kamacite in EH3s. In contrast, graphite lamellae occur in high Ni and low Si kamacite in EH4s. Consequently both Ni and Si were probably controlling factors in the formation of a particular graphite type. The graphite spherules are identical in shape and texture to the spherules produced experimentally by decomposition of cohenite (BRETT, 1967). Hence, we suggest that preexisting cohenite broke down on cooling to produce graphite spherules and render a more Ni-poor kamacite. Since the bulk Ni contents of EH chondrites are comparable (KALLEMEYN and WASSON, 1986), the low Ni-content of kamacite in EH3s is probably the result of formation of perryite as proposed by KALLEMEYN and WASSON (1986). Hence, formation of perryite must have preceded the nucleation of cohenite.

The graphite lamellae in kamacites in St. Marks, Kaidun III, and Indarch were very probably formed by exsolution upon inversion of γFe to αFe due to the low solubility of C in γFe. This may indicate that cohenite did not nucleate in the metal phase in EH4s. ROMIG and GOLDSTEIN (1978) showed that carbides could not be grown during a continuous slow cooling of alloys with high Ni contents (>10 wt%). The Ni contents of kamacites in EH4s is lower than the value given by ROMIG and GOLDSTEIN, however, the presence of several percent of Si may have helped to inhibit the growth of cohenite. ROMIG and GOLDSTEIN (1978) indicate also that the solubility of C in the γFe is lower than previously anticipated. The amount of graphite lamellae found in St. Marks, Kaidun III and Indarch may sometimes reach 30% by volume. The presence of Si probably enhanced the C solubility in the metal phase at high temperature. These interpretations suggest that the Ni content must have been a controlling factor on the formation of the metal graphite assemblages in EH chondrites. Hence, the formation of perryite was critical for changing the original Ni contents in

the metal (KALLEMEYN and WASSON, 1986). Our investigations indicate, however, that perryite forms not only between kamacite and troilite (RAMBALDI *et al.*, 1983), but also as exsolution lamellae (*e.g.* Y-691). Also in this case exsolution of perryite took place before nucleation of cohenite.

Recrystallized troilites with 120° triple junctions are evidence of recrystallization in a long lasting heating event. We suggest that the recrystallization took place in the solar nebula before accretion of the sulfide-bearing objects in the matrix. It is unlikely that recrystallization took place in the parent body because these textures are present in specific fragments, *e.g.* complex metal-sulfide spherules. Other fragments and clasts contain troilite with stress twin lamellae with no signs of recrystallization. The chemical compositions and textures of many of the clasts still preserve records of primordial nebular conditions.

We consider the hydrated Na-, Cr-sulfides in Qingzhen as products of preterrestrial events. The minerals were never observed to occur with caswellsilverite or to replace it. They always occur with daubreelite as oriented intergrowth and with troilite. This intergrowth is strongly suggestive of an exsolution phenomena or epitaxial intergrowth (Fig. 6).

7. A Tentative Scheme for the Evolution of the EH Chondrite Family

Mineral compositions and textural characteristics of members of the EH family reveal systematic and consistent differences indicative of chemical and thermal inhomogeneities in the region of the solar nebula where they were formed.

Both nebular and planetary events may be recognized and placed in a meaningful sequence. Niningerite and oldhamite (and presumably caswellsilverite) were the earlist condensates and acted as accretion nuclei in this highly reduced region of the solar nebula where EH chondrites were formed. Chondrules were formed by melting of material initially depleted in K. The low K content of the chondrules cannot have resulted from the Na/K sulfide fractionation, since both the chondrule glass and caswellsilverite are depleted in K. Nor was the depletion produced by terrestrial weathering as proposed by GROSSMAN *et al.* (1985), since the full complement of K resides in the sulfide fragments in the matrix. Condensation of djerfisherite took place after chondrule formation and definitely after condensation of oldhamite, niningerite, and caswellsilverite.

Evidence for variation in the sulfur and oxygen fugacities is provided by the compositional differences of niningerite, kamacite, and perryite. These differences reveal the presence of three subgroups in the EH family in order of increasing f_{S_2} and decreasing f_{O_2}: (A) Y-691 and Abee, (B) Indarch, and (C) Y-74370, South Oman, Qingzhen, Kota Kota, Kaidun III, and St. Marks. Kamacite compositions clearly indicate that Qingzhen was formed at lower f_{O_2} than Y-691. In the third subgroup four parameters establish an evolution trend among the members: (1) Relative abundance of metal-sulfide clasts, (2) FeS content in niningerite, (3) Graphite-metal intergrowth, and (4) K/Na ratios of djerfisherite. In this subgroup Y-74370 is the least equilibrated and St. Marks the most. By analogy Y-691 is the least equilibrated in the first subgroup.

Compositions of niningerite in the MgS-FeS-MnS ternary diagram contains critical

informations regarding: (a) Temperatures of formation, (b) cooling rates, and (c) thermal episodes to which the meteorites were subjected. Members close to the MgS corner, *e.g.* Y-691, and Y-74370 must have formed at lower temperatures than members with high FeS-contents, *e.g.* Abee, Indarch, and St. Marks. This is in excellent agreement with the experimental results of SKINNER and LUCE (1971) and EHLERS (in preparation, 1988).

Normal zoning in niningerite indicates that the equilibration of the EH members took place during a continuous cooling episode which probably started in the solar nebula and continued after accretion in the parent body. Evidence for planetary metamorphic events was recognized in Qingzhen, Y-691, and Indarch. The reverse zoning in niningerite is unequivocal evidence for these thermal episodes. These events produced the breakdown of djerfisherite (*Qingzhen Reaction*) and the resetting of the ^{40}Ar-^{39}Ar ages. For Qingzhen the event took place at <1.4 Ba ago and in Y-691 at <800 Ma ago. Indarch was subjected to at least two thermal episodes in its early history (EL GORESY and EHLERS, 1987). The last episode was a shock event 4.2 Ba ago.

Acknowledgments

We are grateful to OUYANG Ziyuan, Institute of Geochemistry, Academia Sinica, PRC for the loan of several samples of the Qingzhen meteorite. We acknowledge the help of K. YANAI and Y. IKEDA for supplying us with Y-691 samples. Thanks are also due to S. AGRELL for the loan of a section of South Oman EH chondrite. One of us (A.E.) benefitted from an invitation to attend the 11th Conference on Antarctic Meteorites at Tokyo, March 1986. We are grateful to J. HARTUNG and two anonymous reviewers for their comprehensive reviews.

References

ALBEE, A. T. and RAY, L. (1970): Correction factors for electron probe microanalysis of silicates, oxides, carbonates, phosphates, and sulfates. Anal. Chem., **42**, 1408–1414.

BENCE, A.E. and ALBEE, A.L. (1968): Empirical correction factors for the electron microanalysis of silicates and oxides. J. Geol., **76**, 382–403.

BOCTOR, N.Z. and EL GORESY, A. (1986): Metal-sulfide assemblages in Saint Marks EH5 chondrite (abstract). Meteoritics, **21**, 336–337.

BRETT, R. (1967): Cohenite; Its occurrence and proposed origin. Geochim. Cosmochim. Acta, **31**, 143–159.

CABRI, L.J. (1973): New data on phase relations in the Cu-Fe-S system. Econ. Geol., **68**, 443–454.

EHLERS, K. and EL GORESY, A. (1988): Normal and reverse zoning in niningerite; A novel key parameter to the thermal histories of EH chondrites. Geochim. Cosmochim. Acta (in press).

EL GORESY, A. (1985): The Qingzhen Reaction; Fingerprints of the EH planet? (abstract). Meteoritics, **20**, 639.

EL GORESY, A. and EHLERS, K. (1988): Sphalerites in EH chondrites; Textural relations, compositions, diffusion profiles, and pressure-temperature histories. submitted to Geochim. Cosmochim. Acta.

EL GORESY, A. and KULLERUD, G. (1969): Phase relations in the system Cr-Fe-S. Meteorite Research, ed. by P. M. MILLMAN. Dordrecht, D. Reidel, 638–556 (Astrophysics and Space Science Library, Vol. 12).

EL GORESY, A., YABUKI, H. and PERNICKA, E. (1983): Qingzhen; A tentative alphabet for the enstatite chondrite clan (abstract). Meteoritics, **18**, 293–294.

EL GORESY, A., WOOLUM, D.S., EHLERS, K. and IVANOV, A.V. (1986): Planetary metamorphic events in unequilibrated EH chondrites. Lunar and Planetary Science XVII. Houston, Lunar Planet. Inst., 202–203.

GROSSMAN, J.N., RUBIN A.E., RAMBALDI, E.R., RAJAN, R.S. and WASSON, J.T. (1985): Chondrules in the Qingzhen type-3 enstatite chondrite; Possible precursor components and comparison to ordinary chondrites. Geochim. Cosmochim. Acta, **49**, 1781–1796.

HONDA, M., BERNATOWICZ, T.J. and PODOSEK, F.A. (1983): ^{129}Xe-^{128}Xe and ^{40}Ar-^{39}Ar chronology of two Antarctic enstatite meteorites. Mem. Natl Inst. Polar Res., Spec. Issue, **30**, 275–291.

KALLEMEYN, G.W. and WASSON, J. T. (1986): Compositions of enstatite (EH3, EH4, 5 and EL6) chondrites; Implications regarding their formation. Geochim. Cosmochim. Acta, **50**, 2153–2164.

KEIL, K. (1968). Mineralogical and chemical relationships among enstatite chondrites. J. Geophys. Res., **73**, 6945–6976.

KISSIN, S.A. (1974): Phase relations in portion of the Fe-S system. Ph. D. Thesis, University of Toronto.

KITAMURA, M., WATANABE, S. and MORIMOTO, N. (1986): Pyroxenes in Y-691. Papers Presented to the Eleventh Symposium on Antarctic Meteorites, 25–27 March 1986. Tokyo, Natl Inst. Polar Res., 95–97.

LARIMER, J.W. and BARTHOLOMAY, M. (1979): The role of carbon and oxygen in cosmic gases; Some applications to the chemistry and mineralogy of enstatite chondrites. Geochim. Cosmochim. Acta, **43**, 1455–1466.

LATTIMER, J.M., SCHRAMM, D.N. and GROSSMAN, L. (1978): Condensation in supernova ejecta and isotopic anomalies in meteorites. Astrophys. J., **219**, 230–249.

LUSBY, D., SCOTT, E.R.D. and KEIL, K. (1987): Ubiquitous high-FeO silicates in enstatite chondrites. Proc. Lunar Planet. Sci. Conf., 17th, Pt. 2, E679–E695 (J. Geophys. Res., **92**, B4).

MÜLLER, N. and JESSBERGER, E.K. (1985): Laser ^{40}Ar-^{39}Ar dating of the EH3 Qingzhen chondrite. Lunar and Planetary Science XVI. Houston, Lunar Planet. Inst., 595–596.

NAGAHARA, H. (1985): Petrology of enstatite chondrites, Y-691 (EH3) and Y-74370 (EH4). Papers Presented to the Tenth Symposium on Antarctic Meteorites, 25–27 March 1985. Tokyo, Natl Inst. Polar Res., 12–14.

NAGAHARA, H. and EL GORESY, A. (1984): Yamato-74370; A new enstatite chondrite (EH4). Lunar and Planetary Science XV. Houston, Lunar Planet. Inst., 383–384.

NORRISH, K. and HUTTON, J.T. (1968): An accurate X-ray spectrographic method for the analysis of a wide range of geological samples. Geochim. Cosmochim. Acta, **33**, 431–453.

OKADA, A. (1975): Petrological studies of the Yamato meteorites. Part 1. Mineralogy of the Yamato meteorites. Mem. Natl Inst. Polar Res., Spec. Issue, **5**, 14–66.

OKADA, A., YAGI, K. and SHIMA, M. (1975): Petrological studies of the Yamato meteorites. Part 2. Petrology of the Yamato meteorites. Mem. Natl Inst. Polar Res., Spec. Issue, **5**, 67–82.

OKADA, A., KEIL, K., LEONARD, B.F. and HUTCHEON, I.D. (1985): Schoellhornite, $Na_{0.3}(H_2O)_1[CrS_2]$, a new mineral in the Norton County enstatite achondrite. Am. Mineral., **70**, 638–643.

RAMBALDI, E.R., RAJAN, R.S. and WANG, D. (1983): Chemical and textural study of Qingzhen, a highly unequilibrated enstatite chondrite. Lunar and Planetary Science XIV. Houston, Lunar Planet. Inst., 626–627.

RAMBALDI, E.R., RAJAN, R.S., HOUSLEY, R.M. and WANG, D. (1986): Gallium-bearing sphalerite in a metal-sulfide nodule of the Qingzhen (EH3) chondrite. Meteoritics, **21**, 23–32.

RAMDOHR, P. (1973): The Opaque Minerals in Stony Meteorites. London, Elsevier, 1–244.

ROMIG, A.D., JR. and GOLDSTEIN, J.I. (1978): Determination of the Fe-rich portion of the Fe-Ni-C diagram. Met. Trans., **9A**, 1599–1609.

SEARS, D.W., KALLEMEYN, G.W. and WASSON, J.T. (1982): The compositional classification of chondrites; II. The enstatite chondrite groups. Geochim. Cosmochim. Acta, **46**, 597–608.

SKINNER, B.J. and LUCE, F.D. (1971): Solid solutions of the type (Ca, Mg, Mn, Fe) S and their use as geothermometers for the enstatite chondrites. Am. Mineral., **56**, 1269–1296.

WEAKS, K.S. and SEARS, D.W.G. (1985): Chemical and physical studies of type 3 chondrites—V; The enstatite chondrites. Geochim. Cosmochim. Acta, **49**, 1525–1536.

(Received October 8, 1987; Revised manuscript received December 28, 1987)